to appear in *Encyclopedia of Optical Engineering,*
ed., R. B. Johnson and R. G. Driggers, Marcel Dekker, New York (2002).

VOLUMETRIC STORAGE

Geoffrey W. Burr

IBM Almaden Research Center
650 Harry Road, San Jose, California 95120

Email: *burr@almaden.ibm.com*
Tel: (408) 927–1512
Fax: (408) 927–2100

OUTLINE

INTRODUCTION

One of the reasons that computers have become increasingly important in daily life is because they offer unprecedented access to massive amounts of information. The decreasing cost of storing data and the increasing storage capacities of ever smaller devices have been key enablers of this revolution. Current storage needs are being met because improvements in conventional technologies—such as magnetic hard disk drives, optical disks, and semiconductor memories—have been able to keep pace with the demand for greater and faster storage.

However, there is strong evidence that these surface-storage technologies are approaching fundamental limits that may be difficult to overcome, as ever-smaller bits become less thermally stable and harder to access. Exactly when this limit will be reached remains an open question: some experts predict these barriers will be encountered in a few years, while others believe that conventional technologies can continue to improve for at least five more years. In either case, one or more successors to current data storage technologies will be needed in the near future. An intriguing approach for next generation data-storage is to use light to store information throughout the three-dimensional volume of a material. By distributing data within the volume of the recording medium, it should be possible to achieve far greater storage densities than current technologies can offer.

For instance, the surface storage density accessible with focused beams of light (without near–field techniques) is roughly $1/\lambda^2$ $(1, 2)$. With green light of roughly 0.5 micron wavelength, this should lead to 4 bits/sq. micron or more than 4 Gigabytes (GB) on each side of a 120mm diameter, 1mm thick disk. But by storing data throughout the volume at a density of $1/\lambda^3$, the capacity of the same disk could be increased 2000–fold, to 8 Terabytes (TB). It is interesting to note that the DVD disk standard exceeds this rough estimate of the areal density limit despite using light of slightly longer wavelength. However, no laboratory demonstration of volumetric storage to date has gotten closer than approximately 1% of the $1/\lambda^3$ volumetric density limit (3–7). The vast unrealized potential of volumetric storage, coupled with the hard limitations encroaching upon surface optical (and magnetic) storage, has fueled a large number of research efforts.

This chapter describes and compares several volumetric optical storage approaches that have been proposed and developed in the last decade or so. These include storage of localized bits throughout a volume (accessed either bit–by–bit or in parallel), volume holographic storage, and spectrally selective storage (i.e., spectral hole burning and photon echo storage). Spectrally selective storage, which can each store data in three dimensions plus selectively address by wavelength, is not fundamentally limited to $1/\lambda^3$ and thus might be referred to as four–dimensional data storage.

In the remainder of this section, I describe the generic features common to all three volumetric storage techniques, both to facilitate comparison and to illuminate relevant issues. Each technique is then described in turn, along with its variations, particular storage media and materials requirements, and unique systems issues. In concluding, I compare these volumetric storage techniques and try to give an overview of what each needs to address in order to become a viable next–generation storage technology.

Common features

In its simplest incarnation, a storage device is a black box which takes in user data at some point in time, and which delivers that same data at a later time. Desirable features might include capacity, input and output data rates, latency (the delay between asking for and receiving a desired bit or block of data), cost, system volume, and power consumption. Other defining characteristics might include removability of the storage media, and the ability to erase and rewrite data. High fidelity data retrieval, or conversely, a low probability of data loss through either random errors or catastrophic failure, is an absolute must. The particular bit error rate, as seen by the user (e.g., the user–BER), that is demanded might depend on the intended application of the storage device—the data in the device may be protected by subsequent archival storage, or the device may *be* the archival storage. Whether the black box is a write–once read–many (WORM) or a read–write storage device, the requirement of high fidelity retrieval (at any point in the future) incorporates a desire for long storage lifetime.

Note that density at the media, a metric cited in almost every paper promoting some novel volumetric storage technology, is not mentioned here. Why? Because the only point in acquiring high density is if it can then lead to high capacity—high density in and of itself is insufficient. Picture a storage technology that achieves a density of $1/\lambda^3$ at the media, but which requires a roomful of peripheral equipment for each cubic millimeter of media. Or a technique that can record multiple layers in disk media at a layer spacing of 1 micron, but which is subsequently limited to three layers. Areal density is widely used by the established technologies of magnetic and optical storage, because each evolutionary increase in density leads to commensurate increases in capacity for each well–established form factor. However, when unproven alternate storage technologies focus on density instead of achievable capacity, mismatches in background assumptions often lead to overly inflated initial expectations followed inevitably by entrenched (and perhaps undeserved) disenchantment.

Within the black box storage device, volumetric optical storage technologies tend to have several common features. There is always at least one laser, and a way to modulate incoming data onto this laser beam. An optical system delivers the data–bearing beam to the storage material for recording, and carries it away from the storage material to a detector (or detectors) for readout. This is the point at which volumetric storage diverges from surface optical storage: the recording process must add new data to a volume without obliterating other data already recorded, with the obvious constraint that the laser beam must pass along some contiguous path from an edge into and through the volume. In surface optical storage, the laser beam can illuminate only the bit being accessed; in volumetric storage, the laser beam partially illuminates other, unrelated bits. Like the recording process, the volumetric readout process must retrieve only the desired bits, with tolerable amounts of crosstalk, and the same constraint about access from the edge of the volume. (One way around this constraint is to sandwich layers of the storage material between waveguides which provide access (8)). Channel electronics then reproduce the original binary data from the analog signal(s) detected by the photodetector(s). At this point, something inside the box must change in order that the next storage/retrieval step applies to a different set of data. This might include moving the material, refocusing, steering, or modulating a laser beam, changing the laser wavelength, or changing the media's properties (with electric or magnetic field, for instance) to allow the laser to selectively address a new data set.

Storage capacity then depends on the product of volumetric density (many data sets per unit volume), the accessible volume under each modulator/detector pair, and the number of user bits per data set. Recording rate depends on how long it takes to selectively address the desired data set, and the dwell time of the laser required to store the data. Similarly, readout rate and latency depend on the speed of selective addressing, and the dwell time of the laser required to retrieve the data. The channel electronics add to the latency, but not to the readout rate (unless the electronics are the rate–limiting step). If the storage media is physically moved to selectively address, this often tends to dominate the readout rate and latency. If the storage media is a continuously spinning disk, then the laser often needs to be pulsed (decreasing dwell time) and the latency (the delay to a random data set) can significantly exceed the inverse of the burst readout rate (delay to the next sequentially–placed data set).

In many cases, cost considerations can be broken down into two parts: the cost of the system, and the incremental cost of removable media. The former tends to be dominated by components (laser, modulator, detector, spindles, beam–steerers, optics); the latter usually by finishing costs (cutting, polishing, anti–reflection coatings) rather than by raw material cost. (Of course, since commercialized volumetric storage products are as yet few and far–between, these thoughts are perhaps somewhat speculative). Power consumption budgets also tend to be dominated by peripherals (cryogenics or temperature control if required, spindle, high-voltage modulators) rather than by the detection/modulation electronics or even the laser. Big, inefficient lasers are usually much more painful in terms of cost and size rather than in terms of electrical power consumption.

All of these external factors (capacity, input/output rates and latency, cost, power, and size) are intimately interlinked together, and coupled to the internal consideration of retrieval fidelity. Cost, power, and size can be amortized over large capacity, but large capacity inevitably strains fidelity. Increasing the capacity also affects the speed with which different data sets can be selectively addressed. Media cost couples with media performance (influencing capacity and speed) and media quality (influencing data fidelity). Data fidelity can be addressed with error–correction coding, but only at the cost of additional complexity in channel electronics (both cost, latency, and potential readout rate problems) and reduced capacity (more redundancy means less user data). Judging from the experience of magnetic storage, the only certainty is that no black box will be built with an excessive margin of safety in data fidelity. In general, performance specifications are increased at the cost of fidelity until one reaches the smallest tolerable margin that still satisifies the user–BER constraint.

Stepping back from system design considerations to consider application issues, one finds another tangled web. If some of the features of the ideal black box must be sacrificed during system design, this will have an effect on the eventual market size. For instance, if the stored data doesn't really last forever, or if the recording and readout rates are not comparable, the number of applications that could find a use for the storage device is reduced. Also, people are understandably reluctant to entrust their valuable data to unproven technologies, so finding an initial market may depend on significantly exceeding the performance specifications of competing established storage technologies. In turn, the size of the initial and eventual markets feeds back to the cost and availability of components (particularly those which are not already in wide commercial use through other established technologies), which in turn affect the marketing prospects.

Now that the features and issues of volumetric storage have been introduced in the abstract, the remainder of the chapter turns to specific proposed implementations, beginning with "multilayer" optical storage.

3–D STORAGE OF LOCALIZED BITS

The most straightforward version of volumetric optical storage is the intuitive extension from surface optical storage: localized bits stored not only on the surface but throughout the volume. In relation to the abstract black–box, the modulator is usually the laser itself, and the selective addressing of data–sets is done by focusing the laser beam. Researchers have been exploring several variants of bit–localized storage, which can be roughly grouped into proposals which read one bit at a time, and those which can read multiple bits in parallel. With the former, the laser focuses to single voxels, and reads data out to a single photodetector (or differentially using a few detectors); with the latter, the laser selects a small set of contiguous voxels, and then reads data out to a photodetector array (a CCD or CMOS camera).

Bit–Serial Storage

Extending the CD concept to multiple layers can be done without changing much of the readout hardware (9–11). The focus servo becomes responsible for changing between layers of different depth, in addition to its primary task of locking onto a layer once one is chosen. Crosstalk from other layers (and the possibility of confusion for the focus servo) is minimized by separating layers by a fairly large distance as shown in Figure 1 (this spacing is $\sim$ 55 microns for DVD–ROM (10)). This ensures that when the converging (diverging) beam passes through the nearest neighboring layers, the large spot size covers enough data bits that the loss in transmission due to reflecting pits (and the out-of-focus crosstalk signal in reflection) remains roughly constant (9). If the layers are moved closer together, more crosstalk reaches the detector, and the smaller pool of illuminated data bits means that the statistical variation of random ON and OFF bits can become a significant noise source.

As more layers are added, then the reflectance and transmission of each layer needs to be adjusted so that the signals from each layer are equally detectable. (In the DVD–ROM, this is done by using a gold coating on the top layer and aluminum on the bottom (11).) The signal-to-noise ratio is reduced not only by the lower average signal level, but also by the scattering of the reflected beam as it passes through higher layers on its way back to the detector. As the number of layers increases and the bottom layers move relatively deep into the substrate, a tradeoff emerges between high numerical aperture (needed for tight focusing more than depth of focus since the disk is layered already) and the working distance between the lens and disk surface. Spherical aberration, usually corrected for in the optics, now varies from layer to layer. Without adaptive correction for each layer, this rapidly limits the number of accessible layers: since only one layer can be exactly corrected for (probably in the middle of the disk), the spot-size is maximum at either the top or bottom layers (12). Birefringence of the substrate should also become more problematic as the optical path lengths inside the material increase. Despite these difficulties, early researchers working on multilayer optical storage believed that the number of layers could be increased to 20 simply by increasing the read power (9). For read–write disks, more thought is involved because the read power must remain below the write threshold, and the absorption and recording characteristics as well as the reflectivity of the written state must be individually tuned for each layer. However, by choosing the transmissivity of each

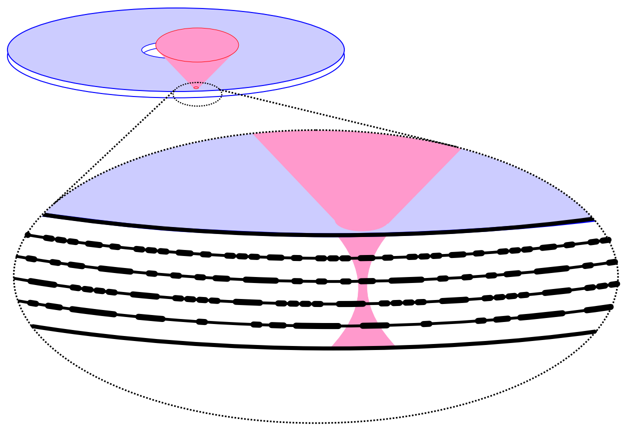

Figure 1: A pre–fabricated disk with multiple layers is accessed from one surface for bit–localized volumetric optical storage.

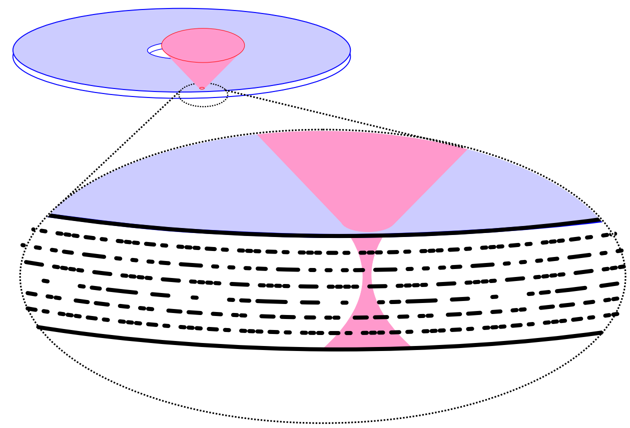

Figure 2: Bits are localized within a initially homogeneous block of media by careful focusing and either confocal imaging, nonlinear material response, or both.

layer carefully, a design point of 20 writable layers with a 100mW laser was found (9). (Note that the media design for just a two layer recordable disk is already quite involved (13–16)).

An additional and important real–world consideration to extending a next–generation–DVD standard beyond two layers is the difficulty of fabricating prerecorded disks with more than two read layers. Currently, while DVD disks can contain as many as four layers, only two layers are read from any surface (i.e., the four–layer disk must be flipped over in a standard one–head drive). So in fabrication, each half of the disk is fabricated with injection molding and is then glued to another half to produce the final disk. If a second data layer is needed on either half, then a 55 micron (±15 micron) thick layer of UV curable polymer is laid down and the bottom layer stamped into this (11, 16). Apparently, one of the main headaches is gluing the substrates together without warping the resulting disk, since commercial DVD drives do not contain a tilt servo to compensate for warped disks (11). Other problems include registering the layers (with same center of rotation) so that a read/write head that is tracking on one layer can move to another and still know which track it will be on, and keeping the layer thicknesses uniform so that the focus servo can always distinguish between layers.

Fluorescent multilayer disks

Other bit–serial methods are variations upon the basic idea of an extended DVD, usually solving one of its basic problems but unavoidably introducing others. For instance, one of the problems with an extended DVD is that the return signal is perturbed by higher layers—this can be avoided by using fluorescent readout, a technique which has been promoted recently for layered disks (17, 18). The readout light is then incoherent and can be wavelength–shifted away from the incoming laser beam so that a filter can block scatter and crosstalk at the laser wavelength from reaching the detector. Of course, this fluorescent dye needs to have the same index of refraction as the substrate, both to avoid the same perturbation of the return signal and to prevent strong reflection of the readout laser. Judging from earlier papers by the proponents of fluorescent multilayer disks (19–25), this technology uses 2–photon fluorescence (i.e., 2–photon absorption followed by fluorescence). Since the fluorescence signal follows the square of the light intensity, the output signal is only efficiently generated where the readout laser beam is focused, which provides the layer discrimination. Both seven (17) and ten (18) layer disks have been publicly demonstrated at CD density (∼0.7 bit/sq. micron), and a 12 layer, 50 GB WORM disk product is under development, to be followed by later write–once products (18). Target specifications include 25 micron layer spacing, DVD–like areal density, and 1x DVD readout speed using a 10mW 532nm laser source (18). A 10GB credit-card sized format is also planned (18).

While the fluorescent multilayer disk removes some of the difficulties in extending localized bit storage to multiple layers, it retains several. The layered disk must still be fabricated carefully as described before, with an additional dye–filling step in which all pits are filled with dye. Assumably to ensure equal filling of all pits, a thin continuous layer of dye exists between pits, which creates a background fluorescence signal (18). After disk fabrication, the desired data is then recorded in these pits with a recording laser, either thermally by destroying the initial fluorescence, or by driving a photochemical reaction which makes the dye in that pit fluoresce (18). Whether this writing process is bit–serial or bit–parallel, the economics of disk fabrication will likely be significantly different than for CDs and DVDs (for which one disk might be stamped every five seconds). The fabrication time will depend strongly on how much writing power is needed: while proponents state that writing can be done with low–power lasers or even LEDs (18), all scientific literature on 2–photon fluorescence has involved high–power lasers, typically ultrashort pulsed lasers capable of high intensities (19–47). Another issue is the readout speed, since the fluorescent dye produces a signal of 1μW (18), much lower than the signal from conventional DVD disks (3–5mW read laser and >50% (>20%) reflectivity for DVD–ROM (DVD–RAM) (10, 16)). These lower signal levels in turn require reduced rotation speed. While aggregate readout rate can be regained by using parallel readout of multiple tracks from the same layer onto a CCD camera (18), this lower rotation rate will still lead to a longer latency than DVD (already one of conventional optical storage's weak points). There has also been discussion of readout of multiple layers through the use of different fluorescing dyes (18), although it is not clear that the required multi–focus objective and multiple filtered readout detectors would be less difficult than simply adding more read heads around the periphery of the disk.

Other methods proposed for improving layered bit–serial localized volumetric optical storage have included the use of optical coherence domain reflectometry (using partially coherent light to get depth discrimination for very weakly reflecting layers) (48), and the use of transparent disks in which abrupt, local changes in layer thickness are detected by measuring the optical path difference between two slightly offset focused beams (differential interference contrast microscopy) (49).

Bit layers in homogeneous media

In contrast with these pre–layered disk schemes, much of the recent scientific literature on localized bit–serial storage has considered the storage of bit layers within initially homogeneous media (Figure 2). Localized–bit volumetric optical data storage has been demonstrated using two–photon fluorescence (21, 22, 25, 32, 40), by bleaching two–photon fluorescence (39,50) , by refractive changes in photochromic (37,43,44,51,52), photopolymer (53,54), photorefractive (4,55–59), and photorefractive polymer (38) materials, and by generating microexplosions in glass through two–photon absorption (5, 36, 41, 45, 60–64). Exposure times have ranged from seconds for photorefractives down to single 100 femtosecond pulses for glass (64).

With large refractive index changes or 2–photon fluorescence, the written data pattern can be read with an ordinary microscope (5, 41, 45, 60, 61, 64). Otherwise, a confocal microscope is usually required to read the data with the desired depth selectivity (4, 37–39, 50, 52, 53, 56, 58, 65–68). The first confocal experiments were performed with a differential interference contrast microscope (as described above) (53). For the more widely–used transmission phase–contrast confocal microscope, it turns out that the optical transfer function does not always provide enough spatial frequency coverage to adequately distinguish localized bits, depending on how the bits were recorded (58, 67). Essentially, such a microscope cannot "see" unslanted reflection gratings of any grating pitch (69). Despite this, several early experiments were performed with special annular optics to prepare the readout focus (56, 65), or a split detector to perform differential measurements (70). A reflection confocal microscope has advantages over the transmission microscope, because the background signal due to scatter and local index inhomogeneities is greatly reduced (37, 68). Having all the optics located on one side of the sample also reduces complexity, and allows a single adjustment of microscope tube length to compensate for spherical aberration (50). Although a reflection phase–contrast microscope has problems similar to the transmission version in covering the spatial frequency band, if the numerical aperture (N.A.) is increased sufficiently and the writing and readout wavelengths chosen carefully, localized bits can be selectively detected (58, 67). Several nice results were obtained this way (4,37,58,68), but unfortunately, the need to have an oil–immersion objective (for N.A.>1.0) limits the general applicability.

Thus research in localized–bit volumetric recording appears to have settled on two–photon processes and fluorescence. This includes one–photon confocal detection of fluorescence changes induced by two–photon absorption (36, 38, 39), and detection with an ordinary microscope of two–photon fluorescence in optically–ablated silica (5, 41, 45). In the former, high intensity CW illumination can also be used to read and write the data (39); in the latter, the ablated bits can also be detected by their large refractive index change (64). Since the photoluminescence, whose origins in optically damaged glasses is not yet well understood (5), can be erased by annealing (41), researchers hope to store two bits per voxel through this method. In addition, by sectioning the glass and measuring the exposed voxels with an atomic–force microscope, Glezer and Mazur found the written marks to be significantly smaller than the optical spot size (61), an effect attributed to self–focusing of the sub–picosecond laser pulse.

Tanaka and Kawata considered the achievable volumetric density for localized bit recording and found that it scaled as $(\mathrm{N.A.})^4$ (66). Factoring in the interplay between high numerical aperture and shorter working distance (i.e., fewer layers), the equivalent areal density of bit–localized volumetric storage (and thus the capacity of a fixed form factor such as a 120mm disk) should scale roughly as $(\mathrm{N.A.})^3$. One of the advantages of recording layers in a homogeneous media is that fabrication issues do not come into play when determining the minimum layer spacing, which should make tighter spacings possible. Thus, the same spherical aberration that would show up for 10 layers at 100 micron layer–spacing would correspond to 200 layers at 5 micron spacing. For media removability, of course, the top layer should still be some distance underneath the surface to avoid problems from surface defects and scratches.

Although many researchers describe their efforts as but a small modification to established CD/DVD technology, there are a number of points where serious effort would be required before products could be developed. For instance, most of these research efforts have concentrated on being able to make and detect small, discrete marks within a volume. In contrast, established surface storage technologies encode data with the distance (and thus disk travel time) between pit edges. This implies that either established technology would need to revamp its modulation coding and signal processing approaches, or the novel volumetric technologies would need to demonstrate the ability to write continuous marks of varying length (without increasing their width in the radial direction or in layer depth). This conventional pulse–width modulation technique seems well–suited to readout and recording with a CW laser (or high–repetition–rate pulsed laser), so that some power is always hitting the disk layer, ready to detect (record) a change. But recording and reading discrete marks efficiently calls for a pulsed laser, because any CW power hitting the disk between marks is essentially wasted.

This brings up an interesting problem concerned with laser pulses and spinning disks. If the marks on a spinning disk are discrete points, then each will arrive under the read/record head at a particular time. However, if the pulsed laser is firing at some predetermined (and fairly low) repetition rate, something must give in order that the laser pulse arrives at the disk simultaneously with the arrival of the mark. Fortunately, since the DVD standard already incorporates a constant linear velocity (in zones for the DVD–RAM standard) to keep the data rate constant (10, 15, 16), it should be possible to synchronize the phase of the disk rotation with the laser pulses when the disk is accelerated or decelerated between tracks. If the same laser is used to record and read marks, the correct spacing between marks is already established. Note that voxels that are sequentially read in time will then most likely be located some distance apart around the circumference of the same radial track within the volume. Although compact pulsed lasers are being researched, using mode–locking in both fiber lasers (71–73) and semiconductors (74, 75), assumably it will be some time before cost, size, and device lifetimes are at acceptable levels.

One final consideration for non–layered bit–serial storage is the difficulty of keeping the focused beam on the right layer and on the right track within that layer. Unlike the pre–layered disks, there is no constant reflection from a surface to auto–focus upon. However, this can be considered as a two–dimensional version of the tracking problems found in magnetic storage. The solution there has been to provide pre–written sectors around the disk with marks designed both to identify the track, and to tell the servo system whether it is straying to the inside or outside of the given track. These ideas could be extended to three–dimensions, either by using two sectors (one for radial error determination and one for depth error determination), or by putting all this information into one

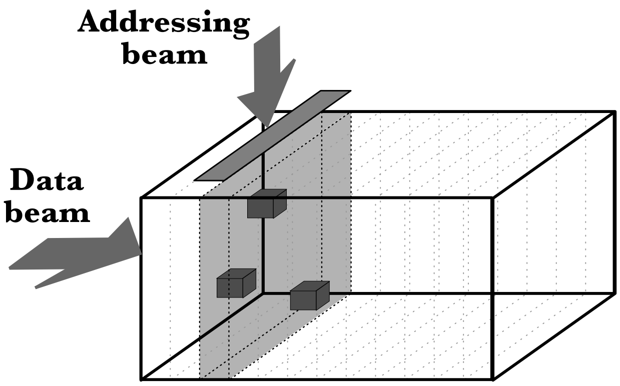

Figure 3: Orthogonal beams used to write and read data in parallel in 3–dimensions using 2–photon fluorescence (After Reference (28)).

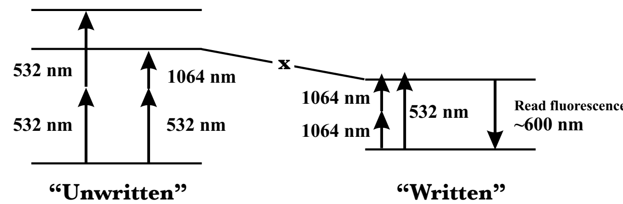

Figure 4: Energy band diagrams for the unwritten and written forms of the fluorescent photochromic material spriobenzopyran (After Reference (28)).

more compact sector.

Bit–Parallel Storage

Parallel readout of 2–photon fluorescence

As mentioned in the description of the fluorescent multilayer disk, moving from bit–serial to bit–parallel access is an attractive way to increase the potential data transfer rates. With two–photon fluorescence readout, a data–set containing many bits can be selected and read out in parallel. A number of papers on bit–parallel two–photon memories have been produced, starting from the initial materials work by Parthenopoulos and Rentzepis (26, 27) and subsequent systems efforts of Esener and co–workers (28–30). In this scheme, the two–photon process is selectively applied to a localized region or spot by applying two beams through orthogonal faces of a cube of material. For bit–serial access, both beams are focused (28); for bit–parallel access, one beam contains a page of information imaged to a plane within the material while the other beam is a cylindrically focused sheet of light illuminating only this image plane from the side (See Figure 3).

Initially, spirobenzopyran embedded in polymer was used because its desirable photochromic behavior (that is, light can induce a change in the molecule's absorption spectrum) was accessible with the fundamental and second harmonic of Nd:YAG lasers (26–28). The energy levels are shown in Figure 4 for the unwritten and written forms of the molecule. The orthogonal arrangement of beams is required because of the potential for two–photon absorption by the green beam alone. By using the green light as the cylindrical addressing beam, the two–photon write process is confined to this illuminated 2–D plane. As shown in Figure 4, written layers can be illuminated either by one– or two–photon fluorescence. Using one–photon fluorescence (green addressing beam for readout) offers more efficiency and does not necessarily imply destructive readout (34). The orthogonal arrangement also provides the opportunity for multi–functional access of database records using the different faces of the storage cube for different database actions (76).

After these initial studies, subsequent materials development then attempted to improve the response of spiropyrans or to find other suitable photochromic materials (19, 20, 29, 31, 33). A list of desired characteristics, adapted from Reference (33), might include:

1. a high two–photon absorption cross–section so that incident light is used efficiently to write information, and/or high doping levels to increase the number of molecules per voxel;
2. the written form of the molecule should have a high fluorescence quantum yield, for sufficient readout signal strength. Note that since the fluorescence is emitted in all directions, only the portion captured by the numerical aperture of the readout optics contributes to the detected signal strength (One proposal for

improving this is to use 3–D photonic bandgap structures at each voxel in order to generate fluorescence only in the desired direction (25));

3. both forms (written and unwritten) of the photochromic molecule should be stable at (and even above) room temperature;

4. high fatigue resistance (i.e., few residual products in the photochemical reactions) for $> 10^6$ write–read–erase cycles;

5. a large separation in absorption and emission spectra so that readout signals can be filtered out, and so that the fluorescence signal does not affect either written or unwritten molecules;

6. nondestructive readout (also linked to the spectral separations);

7. and the capability of being fabricated in low–scatter, high–optical quality samples using simple polymer hosts.

In addition to these rewritable photochromics, write–once materials, composed of organic dyes triggered by photoacid generators, have also been developed (47). For rapid generation of pre–recorded disks, a "stamping" scheme was proposed, using a volume holographic element read with multiple mutually incoherent reference beams to generate the recording optical signals at multiple layers simultaneously (46).

Some of the systems difficulties with this two–photon parallel–access method stem from the media. The low sensitivity of the two–photon process requires high–power pulsed lasers, which means that any optics with an intermediate focus must be enclosed in vacuum (34), and the optics and the spatial light modulator for imposing pixellated data patterns must have high damage thresholds. Despite the high powers, the media still requires hundreds of recording pulses per data plane (34).

Other difficulties are inherent to the system: the need to have a sheet of light implies that the effective width of each data layer will be much larger than the wavelength. Marhic pointed out that this tradeoff between density and transfer rate can actually limit the effective areal density to the same $1/\lambda^2$ limit as surface optical storage (77). Another difficulty is the need to refocus the output detector array onto each data plane to be read (34). This problem can be solved by arranging the data planes in a "turbofan" arrangement, so that each data plane contains the radius of a spinning cylinder or thick disk (42). In this way, the disk rotation brings each data plane to exactly the same position relative to an external read head. The readout light enters the surface of the disk while the fluorescent signals are detected through the curved edge of the disk, using anamorphic optics to correct for the change in path length between disk edge and the different points on the data plane (42). Using such a scheme, twenty–five layers have been recorded and read with a layer spacing of 75 microns (42).

Parallel readout of bacteriorhodopsin

Protein–based bit–parallel volumetric optical data storage has also been proposed (78–80). Although several proteins have been discussed, almost all effort has focused on bacteriorhodopsin, which the *Halobacterium salinarium* bacterium uses to generate energy when the concentration of oxygen is low (79). This protein has a photocycle of states which can be completed in ∼10 ms, for which at least two of the states can be reasonably long–lived (80). Since each state has its own absorption spectrum, binary data storage can be performed by carefully applying or withholding one of the optical frequencies during the photocycle. This has advantages because the lasers can be applied sequentially, and because the optical powers involved can be fairly low (80). One disadvantage is the existence of branches off the photocycle which can lead to material fatigue or crosstalk between bit states. However, a great number of avenues towards material improvement exist, including ambient pH, genetic modifications, and chemical environment. There are several disadvantages in common with the fluorescent 2–photon scheme, including the same density–readout rate tradeoffs because of the diffraction limitations on the parallel–access layer spacing, and the need to refocus a detector array for each plane to be read. Unique problems include the need to use preparatory laser pulses before reading and writing, the need to rewrite data immediately after each read, and the need to perform differential detection to see the absorption changes at the selected layer (and thus retrieve the written data) (80).

HOLOGRAPHIC STORAGE

In contrast to localized–bit recording, where each bit of data is assigned to a particular location within the storage volume, holographic storage distributes data throughout a volume in a delocalized way. A hologram is a recording of the optical interference pattern that forms at the intersection of two coherent optical beams (object and reference—Figure 5(a)). The object beam carries the information to be stored, while the reference beam is designed to be simple to reproduce at a later stage. (A common reference beam is a plane wave: a light beam that propagates without converging or diverging.)

To record a hologram, the reference and object beams are made to overlap in a photosensitive medium, such as a photopolymer (81, 82) or inorganic crystal (81, 83) or even photographic film (84), where the resulting optical interference pattern creates chemical and/or physical changes. As a result, a replica of the interference pattern is stored as a change in absorption, refractive index or thickness. Since the pattern contains information about both the amplitude and the phase of the two light beams, when the recording is illuminated by the readout beam, some of the light is diffracted to "reconstruct" a weak copy of the object beam (Figure 5(b)) (85). If the object beam originally came from a 3–D object, then the reconstructed hologram makes the 3–D object reappear (85).

Although holography was conceived in the late 1940s, it was not considered a potential storage technology until the development of the laser in the 1960s. The resulting rapid development of holography for displaying 3–D images led researchers to realize that potentially, holograms could also store data at a volumetric density of $1/\lambda^3$ (86–88).

In holographic storage, data sets are transferred to and from the storage material as 2–D images composed of thousands of pixels, with each pixel representing a single bit of information. However, no one location in the crystal is responsible for storing that one bit; each bit is distributed throughout the recorded interference fringes. Since an entire "page of data" can be retrieved by a photodetector at the same time, rather than bit-by-bit, the holographic scheme promises fast readout rates as well as high density (81, 89–93). If a thousand holograms, each containing a million pixels, could be retrieved every second, for instance, then the output data rate would reach 1 Gigabit per second. Despite this attractive potential and fairly impressive early progress (94–99), however, research into holographic data storage all but died out in the mid-1970s mostly because of the lack of suitable devices for the input and output of pixelated 2–D data pages.

In the early 1990s, interest in volume-holographic data storage was rekindled (90, 91, 100–103) by the availability of devices that could display and detect 2–D pages, including charge coupled devices (CCD), complementary metal-oxide semiconductor (CMOS) detector chips and small liquid-crystal panels. The wide availability of these devices was made possible by the commercial success of hand-held camcorders, digital cameras, and video projectors. With these components in hand, holographic-storage researchers have begun to demonstrate the potential of this technology in the laboratory (7, 81, 104–113). By using the volume of the media, researchers have experimentally demonstrated that data can be stored at equivalent areal densities of nearly 400 bits/sq. micron (7). (For comparison, a single–layer of a DVD disk stores data at ~ 4.7 bits/sq. micron (114).) A readout rate of 10 Gigabit per second has also been achieved in the laboratory (113).

Holographic Multiplexing

If the hologram is recorded in a thin material—such as the security hologram stamped onto many credit cards—the readout beam can differ in angle or wavelength from the reference beam used for recording the image. The scene will still appear. However, if the hologram is recorded in a thick material, the reconstructed object beam will only appear when the readout beam is nearly identical to the original reference beam.

Since the diffracted wavefront accumulates energy from throughout the thickness of the storage material, a small change in either the wavelength or angle of the readout beam generates enough destructive interference to make

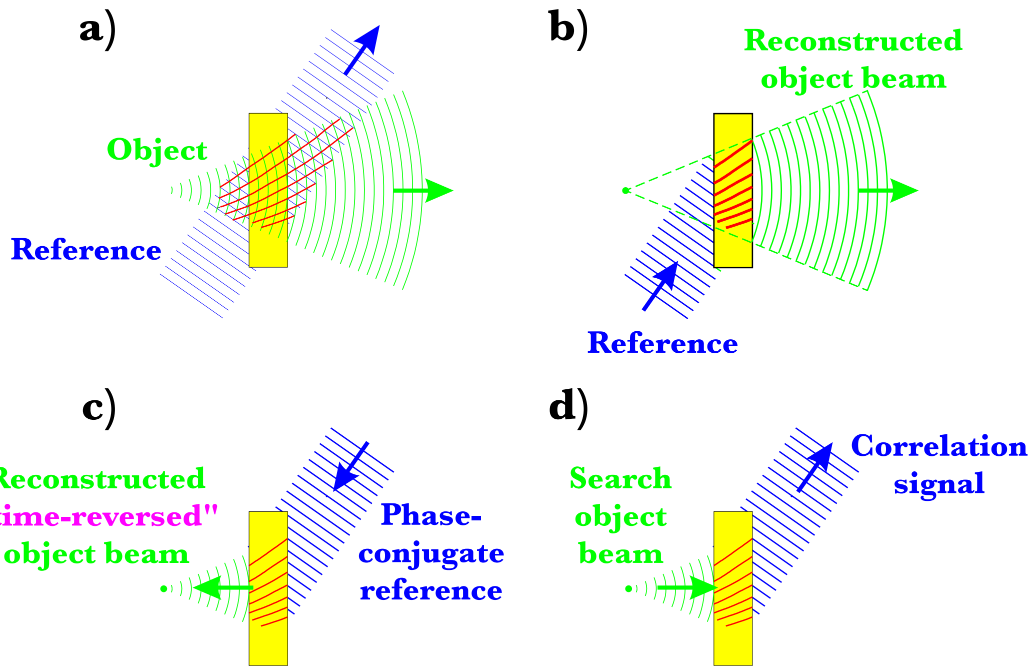

Figure 5: **How to record and read data using holograms:** (a) Holographic storage of a single data bit. The spherical wave from a single pixel interferes with a coherent plane wave in the reference beam. The resulting interference pattern changes the refractive properties of the photosensitive medium. (b) The hologram is read out using the original reference beam, which is diffracted by the stored interference pattern to reconstruct the original spherical wavefront. An image of this beam can be formed on a single detector pixel, resulting in the retrieval of a single bit. (c) The hologram can also be read out by illuminating it with a counter-propagating (or "phase-conjugate") reference beam, which reconstructs a phase-conjugate copy of the original object beam. This beam returns to its original point of origin, where the bit value can be read without requiring a high-quality imaging system (106, 115–121). (d) A third way to retrieve data involves illuminating it with a diverging object beam, which reconstructs the original plane wave reference beam. This beam can be focused onto a detector and provides an optical measurement of the correlation between the stored data and the illuminating object beam (85, 122). This technique can allow one to search the stored data according to its content, rather than according to its address (81, 123–126). (After Reference (93)).

the reconstructed object beam effectively disappear. As the material becomes thicker, accessing a stored volume hologram requires tight tolerances on the stability and repeatability of the wavelength and the angle provided by the laser and readout optics. However, destructive interference also opens up a tremendous opportunity: a small storage volume can now store multiple superimposed holograms, each one distributed throughout the entire volume. The destructive interference allows each of these stored holograms to be selectively accessed with its original reference beam. Several different techniques (81) have been developed to define a set of suitable reference beams by, for example, slightly changing the angle (88, 100), wavelength (127, 128) or phase–front (129–131) of the original light beam. Using so-called "angle multiplexing," as many as 10,000 holograms have been stored in a 1 cm^3 volume (132, 133).

Storing and Retrieving Digital Data

To use volume holography as a storage technology, digital data must be imprinted onto the object beam for recording and then retrieved from the reconstructed object beam during readout (Figure 6).

The device for putting data into the system is called a spatial light modulator (SLM)—a planar array consisting of thousands of pixels. Each pixel is an independent microscopic shutter that can either block or pass light using liquid-crystal or micro-mirror technology. Liquid crystal panels and micro-mirror arrays with 1280×1024 elements

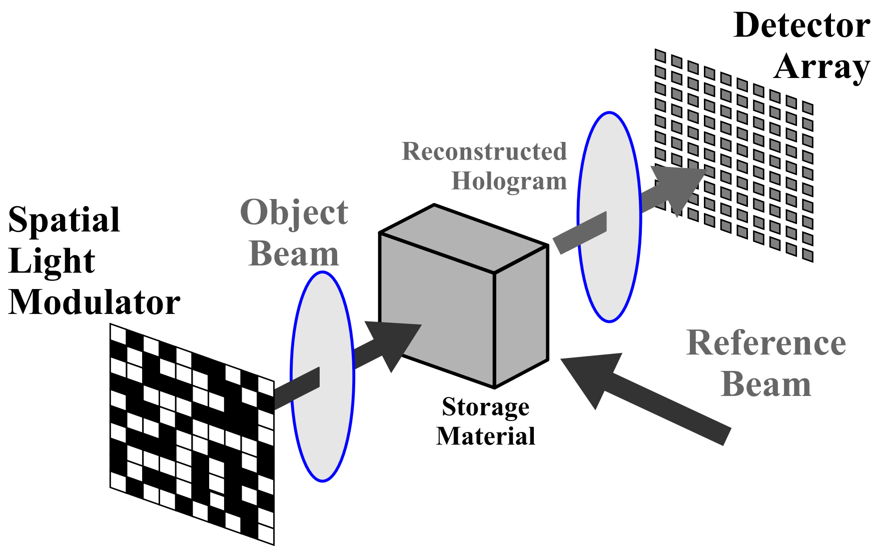

Figure 6: Data are imprinted onto the object beam by shining the light through a pixelated input device called a spatial light modulator. A pair of lenses image the data through the storage material onto a pixelated detector array, such as a charge-coupled device (CCD). A reference beam intersects the object beam in the storage material, allowing the holograms to be stored and retrieved later. (After Reference (93)).

are commercially available due to the success of computer-driven projection displays. The pixels in both types of devices can be refreshed over 1000 times per second, allowing the holographic storage system to reach an input data rate of 1 Gbit per second—assuming that the laser power and material sensitivities permit.

The data are read using an array of detector pixels, such as a CCD camera or CMOS sensor array. The object beam often passes through a set of lenses that image the SLM pixel pattern onto the output pixel array, as shown in Figure 6. To maximize the storage density, the hologram is usually recorded where the object beam is tightly focused. When the hologram is reconstructed by the reference beam, a weak copy of the original object beam continues along the imaging path to the camera, where the optical output can be detected and converted to digital data.

To access holographically-stored data, the correct reference beam must first be directed to the appropriate spot within the storage media. With mechanical access (i.e., a spinning disk), getting to the right spot is slow (long latency), but reading data out can be quick (firing a pulsed laser when the disk is in the right position). While non–mechanical access leads to the possibility for lower latency (fast beamsteerers such as acousto–optic deflectors (81,91,103,105,110) or liquid–crystal beam–steerers (134)), if this is done with a CW laser then the beam must dwell on the hologram, reconstructing it until a sufficient number of photons accumulate to differentiate bright and dark pixels. A frequently mentioned goal is an integration time of about 1 millisecond, which implies that 1000 pages of data can be retrieved per second. If there are 1 million pixels per data page and each pixel stores one bit then the readout rate is 1 Gigabit per second. This goal requires high laser power (at least 1 W), a storage material capable of high diffraction efficiencies, and a detector with a million pixels that can be read out at high frame rates.

Frame rates of 1 kHz have been demonstrated in such "megapixel" CCDs (81), but these are not yet commercially available. Low-noise megapixel CMOS detector arrays that can support 500 frames per second have also been demonstrated (81). Even with these requirements, faster readout and lower latency could be reached by steering the reference beam angle non-mechanically, by using a pulsed laser, and by electronically reading only the desired portion of the detector array. Both the capacity and the readout rate are maximized when each detector pixel is matched to a single pixel on the SLM, but for large pixel arrays this requires careful optical design and alignment (7, 104, 110–112, 135, 136).

Media

Media for holographic storage has long been one of the primary focus points for researchers. Holographic media break into two camps: write–once media, typically to be used as thin (0.2–2 mm) disks and accessed through disk rotation (81, 111, 112, 137–141); and read–write media, typically kept stationary and accessed by beam–steering (90, 91, 101, 103, 105, 110, 132, 142).

Write–once read-many

Materials for writing permanent volume holograms generally involve irreversible photochemical reactions that are triggered by the bright regions of the optical interference pattern. A photopolymer material, for example, polymerizes in response to optical illumination: material diffuses from darker to brighter regions so that short monomer chains can bind together to form long molecular chains (81, 82, 143–151). Because this diffusion process can be phototriggered, sensitivities can be made high enough to support holographic recording with single short pulses (113, 149, 151). However, this opens up worries about regions of the storage volume being inadvertently used up by partial exposure as nearby spots are recorded. In contrast to photopolymers, in a so-called direct-write or photochromic material, the illuminated molecules undergo a local change in their absorption or index of refraction, driven by photochemistry or photo-induced molecular reconfiguration. Examples include photoaddressable polymers (152–155), and binding of absorbers to polymer hosts (such as phenanthraquinone (PQ) to polymethylmethacrylate (PMMA) (156–159)).

Both types of materials are inexpensive to make in bulk, but both can have problems reproducing the object beam faithfully. With the photopolymer, problems arise because the material shrinks during recording, distorting the reconstructed pixelated image (147, 160, 161). The direct-write material responds both to the rapid variations of the interference pattern encoded with data and to long-range brightness variations across the illuminated spot. Such effects distort the reconstructed data pages. These problems can be minimized by careful system design, such as signal–processing techniques that can compensate for shifted and distorted data pages (162), and optical-illumination systems that deliver beams with extremely uniform brightness (163).

One advantage of a photopolymer is that leftover monomers can be polymerized after recording without affecting the holograms. In contrast, a direct-write material requires a separate chemical or optical step after the hologram-recording process to deplete the remaining absorbers. Otherwise, the light from the readout beam would induce further photochemical reactions, reducing the distinction between the bright and dark fringes of the recorded interference pattern and thus erasing the stored holograms. One way around this problem is to use a thermal diffusion process to homogeneously redistribute unexposed absorbers immediately after the holographic recording (156–159, 164), at which point they can no longer "fill in" the hologram. As with photographic film, both photopolymer and direct–write write-once media must be protected from ambient light before use, and tend to lose their effectiveness as they age.

Although problems with shrinkage, scattering and dynamic range remain, recent developments in these write-once materials have overcome previous difficulties with poor optical quality and excessive absorption and led to fairly thick samples (0.5–1 mm). Together with recently developed multiplexing techniques that use "peristrophic" beam rotation (137, 165), spherical (139, 141, 166) or randomly speckled (167–169) reference beams to increase the number of holograms that can be superimposed in thin media, these developments bring "write-once/read-many" holographic storage systems close to the prototype stage.

Read–write

Most erasable holographic materials are inorganic photorefractive crystals doped with transition metals or rare-earth ions (81, 170–174). These crystals are often available in centimeter-thick samples and include lithium niobate (83, 175, 176), strontium barium niobate (177–179), and barium titanate (180–182), doped with iron, cerium, praseodymium, or manganese.

These materials react to the light and dark regions of an interference pattern by transporting and trapping electrons, which subsequently leads to a local change in index of refraction (81, 173). The trapped charge can be rearranged by later illumination, so it is possible to erase recorded holograms and replace them with new ones. This would seem to enable a read-write storage device, where small blocks of data can be written, read, and erased with equal facility. However, the recording rate of photorefractive materials is typically 5–50 times slower than the achievable readout rate. In addition, erasing individual holograms from a small storage volume without affecting the other superimposed holograms is quite involved (183–190). As a result, a holographic storage system built with photorefractive crystals is not a "read-write" system so much as an "erasable write-once, read-many" system. Such a storage device would record data slowly and in large blocks (100–1000MB), but could then provide very rapid access to any small data block (0.1–1MB). These large blocks of data could then be erased and replaced as desired.

The ability of a photorefractive material to erase through charge re-excitation also results in the undesired erasure of stored holograms during normal readout, and even gradual erasure in the dark through thermal excitation (173). Recorded holograms can be "fixed" – i.e. made semi-permanent and resistant to erasure during readout – by separate thermal (94,98,113,191–198) or electronic (178,179,199,200) processes. Unfortunately, this fixing process affects all the stored holograms within a volume simultaneously, and tends to be slow and cumbersome. Other proposed solutions include periodic copying and refreshing of the pixelated data pages (183–190).

An alternate method for achieving non-volatile storage in photorefractive materials is by recording at a wavelength of light which is only absorbed by the crystal in the presence of a third "gating" beam of different wavelength (81, 201–210). This third beam is present only during recording and is switched off while the information is read out, allowing the data to be retrieved without erasure.

Conventional photorefractive materials can be optimized for this gated, two-color recording process by changing the way in which they are fabricated or by adding multiple dopants. For instance, the two-color response of lithium niobate can be enhanced by changing the ratio of lithium to niobium in the compound (206, 208) , or by doping it with both manganese and iron atoms (207, 209, 210). Gated, two-color photorefractive materials have received much attention recently, leading to improvements in both the sensitivity and dynamic range of the materials (increasing both the speed with which data can be written and the capacity) (206–210). Further improvements, however, will be needed before prototypes can be built.

Other read–write materials include photorefractive polymers (211–218), bacteriorhodopsin (219–224), and the DX–center in semiconductor materials (225–228). These materials are difficult to obtain in the thicknesses that would be required for competitive capacities, and also have their own idiosyncrasies. While photorefractive polymers can achieve large index changes very rapidly and provide many avenues for tuning through constituent substitutions, they require large voltages to create the orientational analogue of the electro–optic effect and tend to have fairly short dark lifetimes (seconds to minutes) (217, 218). Bacteriorhodopsin has similar strengths and weaknesses: As described before, it can be tuned by genetic and chemical modifications (219, 224). While an external electric field is not required, the operating wavelengths tend to be tied to the protein's innate photocycle (219,224). Finally, at low temperatures ($<$ 150 K), the persistent photoconductivity exhibited by the "DX" center in semiconductors offers an opportunity for writing strong phase–holograms (225, 226). Photoexcited electrons persist in the conduction band without decaying, leading to large index changes (228). These materials act much like write–once, direct–write saturable materials, which means that readout "fills in" the holograms. However, by raising the temperature, the holograms can be erased since the photoelectrons now have enough thermal energy to make it back to the original ground state (228).

Read–write systems using phase–conjugate readout

High areal density can be achieved in holographic data storage by carefully balancing inter-pixel crosstalk (introduced by the small aperture through which each data page is focused) against the loss of signal associated with recording multiple holograms. An equivalent areal density 80 times larger than that of DVD was recently demonstrated by combining large 'megapel' data pages of 1024x1024 pixels with the short focal length optics needed for high density (7). Careful hardware engineering (81, 163), powerful modulation coding (135, 229), and signal processing to relax alignment and distortion tolerances (162) allowed one thousand pages to be angle–multiplexed without exceeding a raw–BER of 1.1×10^{-3}. This is sufficient to deliver a user-BER of 10^{-12} with the error–correction coding less powerful than that found in CD audio systems. (This assumes that raw byte errors can be uniformly distributed across the error–correction codewords through suitable interleaving (230).) Given the 5.5mm hologram thickness, this result corresponds to 1.1% of the well-known theoretical volumetric density limit of $1/\lambda^3$.

However, extending read-write holographic storage to high capacity without sacrificing fast access means that this same high density must be achieved at many storage locations without moving the storage media. The correspondingly greater demands on optical imaging performance limit the capacity achievable by simply designing better lenses to commercially uninteresting values. However, several researchers have long proposed bypassing these imaging constraints with phase-conjugate readout (106, 115–120).

Once a hologram is recorded, the wavefront reconstructed by a phase-conjugate readout beam will retrace the path of the incoming object beam in reverse, canceling out any accumulated phase errors from lens aberrations or material imperfections. This allows data pages to be retrieved with high fidelity using image confinement in fiber–type media (115–119), an inexpensive lens, or even without imaging lenses for an extremely compact system (106, 120).

However, many pairs of phase-conjugate reference beams are needed to read the many different holograms recorded within the same volume – and maintaining these beams over long periods of time would be impossible from a practical point of view. This problem can be solved by separating the phase-conjugation and hologram storage processes into two successive steps with a 'buffer' hologram (121). Holograms can then easily be multiplexed at a large number of separate storage locations using only one SLM and one detector array. With gated, two–color media, the long–term storage material does not absorb the information–bearing beam until the gating light is present (121). With the phase–conjugate readout, total internal reflection could be used to confine the image–bearing beam within a small cross–section without sacrificing the ability to retrieve this image at the detector array (115–119, 121). Finally, since such a system only requires a single pair of phase-conjugate beams, it can generate these beams either by carefully aligning two fixed beams or with a self–pumped phase-conjugate mirror (121).

The successful use of phase-conjugation in holographic storage should enable compact and affordable high-capacity systems, with only a moderate increase in the overall system complexity. However, such systems still await a recording material that supports both read-write access and nonvolatile storage (202, 207, 208). There are other serious issues that must be addressed before commercialization, such as thermal stability (as the media expands or contracts with temperature, the interference patterns change spacing and orientation), and mechanical and laser stability (media and interference fringes must not move during exposures, and motion afterwards can cause the reconstructed optical signals to veer off their assigned detector pixels). In part, this becomes easier as exposure times decrease through improvements in material sensitivity and increases in available laser power. In addition, it is unlikely that any read–write holographic storage material will be truly non–volatile: most likely the data will slowly fade over several months or years due to thermal effects (slow excitation from electron traps, diffusion of compensating ions) or through residual absorption. So while blocks of read–write media may be removable from the read/write head (which enables something like a petabyte jukebox), the media will probably need to remain within the jukebox so that data can be periodically refreshed.

Write–once systems using spinning disks

In contrast to read–write holographic systems, progress in write–once materials research (especially photopolymers (81, 231)) has brought write–once systems to the stage where people are working on prototypes. Now the long–held conventional wisdom that the only thing between researchers and products was the material will finally be challenged.

Beyond the problems of perfecting the media (in characteristics such as dynamic range, scatter, sensitivity, shelf–life before and after recording, and thermal expansion properties) are the systems engineering issues of building robust holographic data storage devices around a spinning disk format. What makes this even trickier is that the obvious application areas (low–cost data archiving, possible next–generation distribution format for data and multimedia) call for inexpensive and robust disk readers (as well as cheap media). The first systems problem is the interplay between high rotation speed (needed for low latency) and the need for a high–power, compact pulsed laser to read and write with single pulses. And then there are the difficulties of getting the pulse to the right spot (tracking, focusing, synchronizing pulses to disk rotation), and getting the reconstructed data page to the detector array (compensating for tracking, tilt, disk jitter). Zhou et. al. have demonstrated tracking for low density holographic disks (81, 112). They showed both tracking and tilt compensation: the former by measuring the data page rotation to synchronize the beam shutter (on a CW laser), and the latter by tuning the reference beam angle so that data pages landed squarely on the pixelated detector array (81, 112).

To get high density, one must come in with the reference beam from a wide spread of angles, so good antireflection coatings are needed to keep power from being lost in Fresnel reflections (thus increasing media cost). Also for high density and to keep aberrations in the imaging system low, the object beam probably needs to come in normal to the disk through a short–working–distance optical system, further complicating the delivery of writing beams. Although a read–only transmission–geometry head can avoid having to slip the reference beam past the object beam delivery optics, transmission geometry implies that the read head is split into two parts on either side of the rotating disk (and both sides must be aligned).

Several novel multiplexing methods have been developed to allow holograms to be superimposed very densely, even in thin disks. High density can be reached with "peristrophic" multiplexing, at the cost of a fairly complicated read head that rotates the reference beam around the normal to the disk surface (137, 165). In contrast, by using either a spherical (139, 141, 166) or a randomly speckled (167–169) reference beam, the motion of the spinning disk can allow the reference beam to selectively reconstruct stored holograms with an extremely simple read heads. If this "shift" multiplexing is done with a spherical reference beam, then holograms can be packed densely along one line (i.e., along the track), but only sparsely along the orthogonal direction (tracks must be widely–spaced) (139, 141). Speckle–shift, or correlation, multiplexing using a random phase plate or diffuser (113, 167–169) can allow dense packing in both radial and along–track dimensions, but this advantage does not come for free. Essentially, the size of the random speckles determines the disk motion needed to make each hologram disappear through destructive interference (167, 168). This should be small to maximize density, but not as small as the innate disk wobble and jitter of an inexpensive disk and spindle. On the other hand, the destructive interference depends on the number of random speckles that are spatially integrated over as the reconstructed hologram transits the thickness of the disk. So while smaller speckle leads to better inter–page crosstalk SNR, it also makes the readout conditions so selective that holograms might not be reliably found with inexpensive components.

These systems difficulties do not prevent one from building systems that can write and read holograms on spinning disks—several working demonstrations have been shown (81, 111–113). For instance, Orlov et. al., working at Stanford on the final systems demonstrator for the DARPA–sponsored HDSS (Holographic Data Storage Systems) program, built a system capable of 10 Gbit/second optical readout, and 1 Gbit/second end-to-end electronic readout, at greater than DVD areal densities on a disk spinning at >300 RPM (113). The spindle was so accurate that holograms could be incrementally recorded over several rotations (i.e., the accuracy and repeatability were at interferometric levels) (113). However, any commercial product will need to use much smaller and cheaper components, without sacrificing the high density, the fast readout rate, and the ability to robustly write and read holograms on the fly.

An alternate approach to wavelength–multiplexing is to use micro–holograms (232–236). Here each micro–hologram occupies a few square microns of surface area, and extend throughout the thickness of the disk. Multiple bits of data are written at each microhologram by means of reflection gratings, which can be read out by normal wavelength or angle multiplexing (234), or by passive wavelength multiplexing (white light in, colored light out containing data) (235–237). The beams are confined either by the focussed beam itself within a thin film (234), or by a micro–fiber within the material (235). Similar ideas of wavelength–coding (by holograms or dielectric

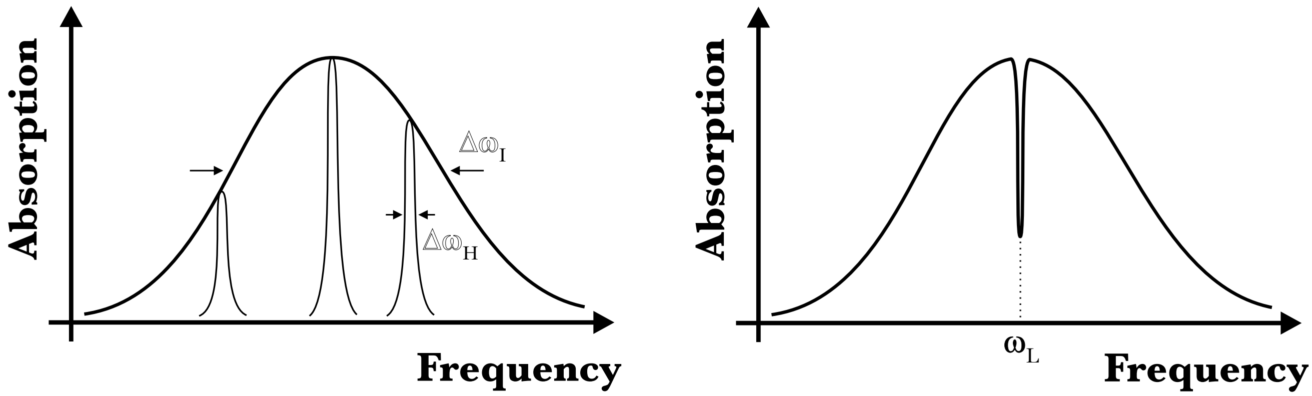

Figure 7: (a) Inhomogeneously–broadened absorption spectrum. (b) After illumination with a narrowband laser at ω_L, a persistent spectral hole has been "burned" into the absorption spectrum. (After Reference (245)).

stack reflectors) at each voxel of a prefabricated multilayer disk have also been proposed (232, 233).

SPECTRALLY–SELECTIVE DATA STORAGE

So far, we have discussed volumetric optical storage, in which data is stored throughout three spatial dimensions. While wavelength multiplexing of volume holograms was discussed, this was essentially another method of selectively accessing the 3D–spatially–distributed data. Once all three dimensions of the storage material have been used via angle multiplexing, any new holograms added with a new wavelength cannot avoid crosstalk from the existing holograms.

Is there a way to extend optical storage beyond $1/\lambda^3$, so that the laser wavelength could be used as an fourth dimension to the storage address? Such spectrally–selective storage is possible in several ways. Several researchers have proposed adding a wavelength dimension to 2–D surface optical storage by using color centers (238, 239), metal–film resonances (240–242), and photochromics (243, 244). These techniques hope to extend surface optical storage by about an order of magnitude, but in each case are probably extendable to localized–bit volumetric storage as well. With color centers, the difficulty is getting the absorption bands narrow enough, both to provide many independent colors and to allow sufficient signal (on other wavelengths) to pass through to other layers (238, 239). With metal–film resonance, the wavelength selectivity depends on the size and shape of the deposited metal bit (as well as the type of metal) (240–242), which implies that fabrication tolerances are going to be tight.

An older technique with the raw potential for several orders of magnitude improvement upon 3–D volumetric storage is the use of persistent spectral hole–burning.

Spectral Hole Burning

For some absorbing molecules doped into a transparent host, an interesting thing can happen to the portion of the absorption spectra introduced by the dopant. By illuminating the material with a highly–monochromatic laser, one can burn a narrow hole in the absorption spectrum at that wavelength (Figure 7). These hosts can be crystalline (246–250), organic (251–253), or glasses (254, 255); the molecules can be rare–earth ions, color centers, or other absorbing molecules (256). The particular resonance frequency of each dopant molecule depends in part on its local neighborhood, with a frequency width referred to as the homogeneously–broadened linewidth, $\delta\omega_H$. The spectral hole comes about when incident light resonates with the subset of molecules whose local environment has shifted their homogeneous linewidths to that frequency—and all the other molecules, with different local environments and thus different resonance frequencies, ignore the laser radiation. This spectral hole only becomes persistent when there is some other "written" state for the photoexcited molecule to decay to other than the original ground state—this can either be a metastable trap level between the conduction and valence band (257–260), a different molecular orientation (259–261), a slightly different ground state level (hyperfine level) (249, 259, 260, 262, 263), or other photochemical or photophysical change in either the absorber or its local environment (256).

This raises the possibility of storing data in the frequency dimension in addition to storage throughout three dimensions. This has been the subject of research for several decades (246, 259, 260, 264–270), a field which has branched out into several sub–disciplines, each aiming to take advantage of a different aspect of the duality between the temporal and frequency domains. First we discuss the simple idea of adding a frequency–selective dimension to localized–bit recording, so that each voxel stores much more than just one bit.

How much more depends on how many independent spectral holes can be burned at one spot. The overall absorption spectrum due to all doped molecules is the sum of all the homogeneous linewidths of the individual molecules, referred to as the inhomogeneous linewidth, $\delta\omega_I$. Unfortunately, the ratio between the overall inhomogeneous and the individual homogeneous linewidths usually doesn't get to interesting values until the temperature is reduced to cryogenic levels ($\sim$ 4K). (There are a few examples of burning multiple holes at 77K (271,272)). The low temperature makes mechanical motion of the media to access spatial locations much less practical, leaving mechanical and nonmechanical scanning of the laser beam. A frequency–tunable laser is required—and tuning over a wide range with a mechanically rotated grating (273, 274) or by temperature tuning a semiconductor diode laser (275, 276) can be slow (a narrow range can be covered rapidly by an intracavity electro–optic element (277–279)). To reduce the impact of time delays associated with changing the laser wavelength, one can try to arrange both data and requests so that large contiguous blocks of data can be read out with one frequency. Typical values for the inhomogeneous linewidth vary from 500 MHz up to 10 GHz for inorganic crystals (corresponding to a wavelength change of just 0.02 nm) (260) up to 10 THz for dye–doped polymers (280), while the homogeneous linewidth can be as low as 100 Hz (263). References (256,259,260) review several persistent spectral hole burning materials. Another consideration is the location of the new resonance frequency of the molecules that were photoexcited to generate each spectral hole. If these new frequencies are still within the inhomogeneous band ("anti-holes" (256,281)), then this limits the number of spectral holes that can be independently stored. Also, since the resonance frequency of the spectral holes (both burned and unburned) depends on local environment, as more and more holes are burned, the likelihood of affecting this local neighborhood increases, leading to excitation–induced frequency shifts and broadening of the effective homogeneous linewidth (282–286) from its theoretical best full–width–at–half–maxima of 2 $\delta\omega_H$ (256). Other phenomena that can lead to broader holes (and thus less stored data per voxel) are power broadening (256, 287–290), spectral diffusion from too many doped molecules (291), photochemical broadening from overly–efficient hole burning (291), and phonon scattering as the temperature increases (256).

Then there is the question of the persistence of the spectral hole—in most of the demonstrated materials systems, the "written" state usually decays back to the original state, filling the spectral hole, in a relaxation time which can vary from a few milliseconds to hours or days (251, 256, 259, 263, 292, 293). And since the stored data must be read by measuring the absorption, the same volatility problem suffered by photorefractive holographic media shows up: the read process tends to erase the stored data. These problems imply that spectral hole burning memories are best suited as cache or otherwise temporary storage (260, 270). However, the ability to use rapid nonmechanical access (such as 10-100μsec access offered by acousto–optic deflectors) presents the opportunity to fill the large access time gap between DRAM ($\sim$100 nsec) and magnetic hard drives ($\sim$ 5 msec).

Such optical cache memories could have fairly impressive capacities even when the frequency dimension is added to only 2–dimensional surface storage. This is because the ratio between the inhomogeneous and homogeneous linewidths can be $> 10^6$, offering more of a capacity advantage over a thin disk than simple volumetric storage can (256, 259, 260). For instance, Murase et. al. showed that the theoretical capacity with spectral hole burning could be 260 bits/sq. micron with 600nm light, a readout rate of 100Mbit/second, and a $\delta\omega_I/\delta\omega_H$ ratio of only 1000 (294). It would then seem logical that adding frequency–selective storage to localized–bit *volumetric* storage would then provide four–dimensional storage. However, the 2–D + frequency disk has usually already used the volumetric dimension, in order to fill the illuminated spot with enough molecules for each spectral hole (because increasing the number of spectral holes means fewer molecules in each). Conventional localized–bit volumetric storage achieves voxel selectivity by focusing and using material systems that respond nonlinearly to the high intensity. With spectral hole burning, the duration and power of the recording optical exposure has to be carefully adjusted so that the depth of the spectral hole is maximized (256,259,268,291,295). Less exposure and not enough of the molecules have absorbed light; more and too many of them have been resonantly driven back down to the original ground state (and the hole broadens). Adjusting this exposure across a tightly focused beam would be difficult.

There is also the problem of volumetric selectivity—how to burn the spectral holes just at one localized volumetric location without affecting the entire illuminated volume? One way to do this is to use photon–gated spectral hole burning, where the excitation of molecules can be done in two steps using a metastable intermediate level (259, 296–302), similar to the gated photorefractive materials described earlier. Gated spectral–hole burning materials thus allow the readout process to be nonvolatile. However, the gated materials found so far tend to have shorter lifetimes and lower sensitivities than single–step persistent spectral hole burning materials (260). Moerner and Levenson showed that single–photon processes could be used for persistent spectral hole burning memories, provided that the right combination of high quantum efficiency, high doping levels, and *low* absorption cross–sections can be found (291). Essentially, if the molecules absorb photons too readily, then it will be too hard to detect the hole without erasing it. However, when a photon is finally absorbed, it must be very efficient at contributing to the spectral hole.

Another way to use the spatial depth of the material is to combine persistent spectral hole burning with volume holography, recording combined space–and–wavelength holograms (289, 290, 303–310). Here each subset of molecules can be used to record combined absorption–and–phase holograms (289), because the Kramers–Kronig relationship (287) implies that a change in absorption will be accompanied by changes in the index of refraction at wavelengths both slightly above and below the absorption resonance. Writing a spatial hologram with spectral holes is a convenient way to detect faint spectral holes (303), because no spectral hole means no light diffracted to the optical detector. This zero–background detection provides advantages over trying to directly detect the very small relative changes in absorption coefficient representing a faint spectral hole via various modulation techniques (245, 259, 311–313).

By modulating the local environments of the molecules through the Stark effect, electric field can also be used along with wavelength to multiplex data–bearing holograms (303, 306). Here the same wavelength interacts with different subsets of molecules, accessed by tuning the Stark shift. Similar to wavelength and angle multiplexing in regular volume holography, however, electric field cannot add another dimension to the data storage, but merely provides another avenue for fully exploiting the spectral dimension (290). That is, once a subset of molecules has data encoded into it by electric–field multiplexing, one cannot expect to then re–write this same subset at a different wavelength under zero electric field.

Because both the phase and amplitude "version" of the hologram diffract light, and because the index of refraction changes occupy a larger range of wavelengths around the center of the spectral hole, there is more crosstalk between these spatial holograms than between ordinary spectral holes. However, by stepping the phase between reference and object between exposures, this crosstalk between spectrally–adjacent holograms can be reduced (305, 306), and by sweeping phase and frequency during recording, one can even control the diffraction orders of thin holograms (307). And by double exposing a hologram at two wavelengths that are slightly offset symmetrically around the desired readout wavelength, a pure phase hologram can be recorded that offers less crosstalk between holograms (290). Essentially, the wavelength spacing is chosen such that the absorption contributions subtract and the index (or phase) contributions add. Using this technique, as many as 12,000 space–and–wavelength holograms have been recorded in a single 2.5cm $\times$ 2.5cm spot on a thin sample of dye–doped polymer film (310).

In general, the difficulty of satisfying the various materials characteristics simultaneously has been one of the factors limiting the development of spectrally–selective memories (256, 259, 260, 291, 295, 314). These desired characteristics might include:

1. A large ratio of inhomogeneous to homogeneous linewidths;
2. A center wavelength accessible by a convenient laser source;
3. High sensitivity (absorption cross–section or oscillator strength of the excited transition, combined with high

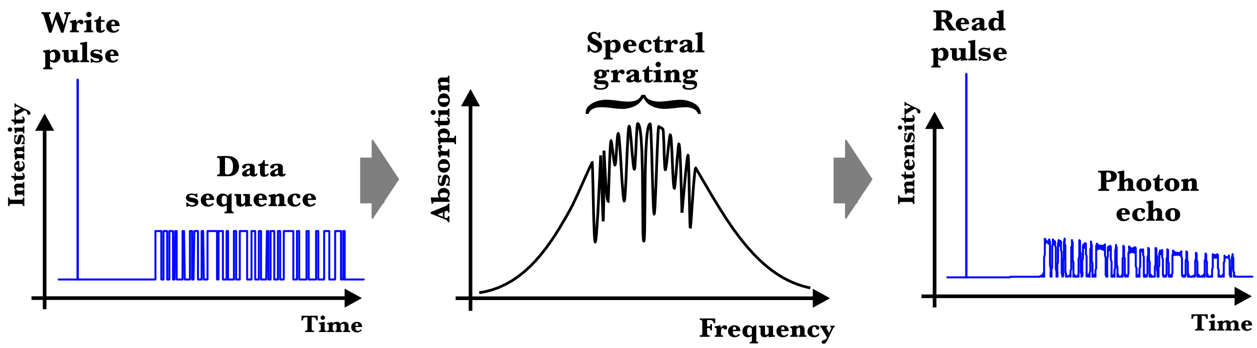

Figure 8: Illuminating a spectrally–sensitive material with a brief reference pulse and a temporal data sequence records a spectral hologram into the inhomogeneously–broadened absorption spectrum. Illumination with an identical brief reference pulse then replays the original temporal data sequence as a "photon–echo."

quantum efficiency for transfer into the persistent state) for efficient recording (no 'bottleneck' states (259));

4. A lack of mechanisms which broaden the recorded spectral holes;

5. Long storage lifetime;

6. Gated recording if possible for nondestructive readout—if not, then the proper combination of high doping, high quantum efficiency, and *low* absorption cross–section (291);

7. A large homogeneous linewidth (in absolute units).

This last desired characteristic might not seem necessary, since the number of stored spectral holes would seem to scale with the ratio between the inhomogeneous and homogeneous linewidths and not depend on the absolute linewidth. In fact, the larger the inhomogeneous linewidth, the wider the required tuning range of the frequency–agile laser source. The two biggest problems with recording and detection of persistent spectral holes, however, are related to the narrow homogeneous linewidth. As this linewidth decreases, the required frequency stability of the laser must follow so that these narrow holes can be written and detected. For example, a typical single–mode CW research–grade ion laser might have a coherence length of 30 meters, long enough that building a simple asymmetric interferometer to measure it is somewhat difficult on an optical table. However, this coherence length corresponds to a linewidth of 10 MHz. If the homogeneous linewidth is much lower (perhaps even 100Hz), then the laser must be carefully stabilized externally in order to fully exploit the spectral storage dimension. Methods include using a high–finesse cavity or interferometer (315–318), locking to an atomic absorption line (319, 320), or even frequency–locking to a spectral hole (321–323).

The second problem with narrow homogeneous linewidth stems from the underlying time–frequency duality. If a spectral hole is only $\Delta\omega$ =100Hz wide, then by definition the recording light must expose the molecules for at least $1/\Delta\omega$ =10 milliseconds in order to avoid containing frequency components outside the desired 100Hz band (and thus exciting the molecules of neighboring spectral slots as well). This creates an undesirable tradeoff between maximal capacity and maximal transfer rate (268). Unfortunately, the materials with the best ratios of inhomogeneous to homogeneous linewidth seem to produce them by having very narrow homogeneous line (rather than via a broader inhomogeneous line) (260).

However, researchers have known about this constraint for many years and have developed an entire family of techniques for addressing the same spectral hole burning materials through the other side of the same time–frequency duality: by storing data in the temporal dimension as "photon echoes (268, 324)."

Photon–Echo Storage

Photon–echo storage, often simply called time–domain storage, can be thought of as the temporal analogue to volume holography (325). In volume holography, data are spatially modulated onto a laser beam; in photon–echo storage, data are input and output as temporal sequences modulated onto the recording laser beam. Just as the interference between two beams creates a spatial pattern to be recorded throughout a volume, the interference between two temporal sequences creates a spectral interference pattern which is then recorded by the same homogeneous linewidths of the same spectral hole burning material (260, 268, 295, 326). In the same way that the phase and amplitude of the spatial wavefront is preserved in an intensity–only recording through the beat frequency, the phase and amplitude of the spectral pattern is preserved in the absorption–only recording of spectral holes (268, 327). Since phase in any function (here the spectral pattern) results in a shift in its Fourier transform (the time domain), the spectral holes have essentially recorded the time delays of the input signal (295, 328) (Figure 8). In fact, it is possible to sequentially burn holes at different frequencies and then read the resulting synthetic photon echo (329, 330), or vice versa (327, 331).

This preservation of time relationships holds for as long as the molecules respond coherently to the incoming radiation. That is, the two–level atomic system distributes the electron population in such a way that the time delay since the excitation is remembered, until the "memory" of the individual molecules begin to differ (decohere). For this same reason, the two temporal sequences do not need to be simultaneous. In fact, changing the order of the pulses makes it possible to time–reverse the temporal data sequence (268, 269, 332, 333), and multiple pulses can be accumulated to make the signal easier to detect (334–337). The dephasing or decoherence time is roughly related to the inverse of the narrow homogeneous linewidth, and thus sets the maximum length of the temporal signal (256, 259, 268). The shortest possible temporal feature is then inversely related to the broad inhomogeneous linewidth, since shorter temporal features would lead to spectral features which are not absorbed by the material. The total amount of data is then still set by the ratio of $\delta\omega_I$ to $\delta\omega_H$. The advantage of the photon–echo technique is that the potential data transfer rate is now tied to the inhomogeneous linewidth, which can be several orders of magnitude faster than the homogeneous linewidth (259, 260).

The readout of a hologram is mathematically the correlation of three functions: the object, the reference, and the readout beam (pulse sequence). The ability to perform correlations of temporally arranged data makes it possible to do photon–echo signal processing, for applications such as time–delay generation and other radar signal processing functions (328, 338–341), header decoding and other processing useful for telecommunications (342–345), general pattern recognition and signal processing of temporal data (338–340,346–351), and even optical logic (352, 353). The telecommunications applications have been greatly advanced by recent improvements in materials that can burn spectral holes near the 1.5 micron band used by long–haul telecomm (345, 354).

To be able to retrieve an object pulse sequence, two of the three functions in this triple correlation need to disappear into a delta function. The most obvious way to do this is with two pulses so brief as to be delta functions themselves (268, 269). In terms of frequency space, one only needs to cover the entire inhomogeneous linewidth. However, the need to deliver a certain amount of power means that these pulses are difficult to repeatedly and accurately generate, and when they arrive at the storage material they tend to drive the material into saturation. Since the material no longer responds linearly to the object pulse, the output data will be severely distorted. One solution to this problem is to use a reference (and readout) pulse that is swept (or chirped) at some rate across some portion of the inhomogeneous linewidth (278, 279, 325, 355, 356). As long as everything occurs within the homogeneous dephasing time, the molecules across all the illuminated homogeneous linewidths will respond. The readout pulse needs to have the same chirp rate as the writing pulse, so the pulse generation problem has been replaced by the need to produce repeatable frequency chirps. So fairly good laser stability is still required for photon–echo storage, especially if the homogeneous linewidth is narrow. In addition to sweeping frequency, one can simultaneously sweep the illuminated spot across some small part of the volume (357). Although this can complicate things if the reference and object pulses have to arrive on separate beams, this helps reduce the fraction of the inhomogeneous linewidth that is excited at any one instant at any one location, thus reducing the effects of excitation–induced frequency shifts which would otherwise greatly increase the effective homogeneous linewidth (282–286).

After solving the troubles caused by the sharp temporal reference pulse, there may still be sharp features in the frequency spectrum of the data pulse caused by amplitude–only modulation. So several techniques have been developed for phase–modulating or otherwise smoothing the spectrum of the temporal data sequence (358–362). (Similar techniques, using diffusers, random phase–masks, or other optical elements (363–365) are often needed in the spatial domain for regular volume holography.) The signal level of the photon echo can be increased by optimizing the absorption and thus the number of contributing molecules (366–368) or by subsequent amplification (369).

In addition to the recording of a temporal interference pattern, it is possible to simultaneously record a spatial interference pattern (302, 326, 330–333, 370–373). Such spatial–spectral holography offers the opportunity for true four–dimensional storage, as well as offering parallelism to the temporal signal processing applications (343, 349, 370). Interestingly, while a large inhomogeneous linewidth was useful for spectral hole burning (because then wider spectral holes could be written without reducing the total number of holes), if the inhomogeneous linewidth gets too broad in photon–echo storage, then the usable bandwidth of the material is not easily accessible with the modulators available today. One way around this might be to use several widely separated laser wavelengths to cover the inhomogeneous linewidth, with the bandwidth between each covered by time–domain techniques (325, 371).

Ultrafast optics

In addition to the use of spectrally–sensitive materials, it is possible to use spatial light modulators and room–temperature nonlinear optical materials to process and store time–domain information (374–379). A incident femtosecond pulse or pulse train can be distributed into its constituent frequency components by a simple grating, thus mapping frequency into angle (374). A 4–F system (two lenses separated by the sum of their focal lengths) can then separate each ray angle into a spatial position within the central shared focal plane, where phase– and amplitude–modulation can be performed. A second lens and grating serve to recombine the frequency components into the temporal pulse dictated by the Fourier mask or spatial light modulator in the center plane (374). By introducing a second pulse, a spatial hologram can be recorded at the center plane in order to store temporal optical waveforms (375). By using nonlinear optical effects, one can control ultrafast wavefroms in real–time through conversion of spatial–domain images (380–382). This provides an avenue for using the same techniques of spatial holographic data storage, with the data input and output in temporal rather than spatial form.

CONCLUSIONS AND OUTLOOK

This chapter has surveyed three main variants of volumetric storage: localized–bit, holographic, and spectrally–selective storage. Each has shown promise in initial research studies, and each shows the potential to significantly out–perform conventional storage technologies in at least one of the desirable 'black–box' specifications (capacity, input and output data rates, latency, cost, system volume, and power consumption).

Serial storage of localized–bits throughout a multilayered disk offers to increase the capacity of a standard optical disk with moderate changes to the readout optics (and the disk fabrication infrastructure). Parallel readout then can be added to increase readout rate, with the degree of modification to conventional readout systems depending on the degree of parallelism.

Holographic storage, which distributes or delocalizes data throughout a volume with interference fringes, can take two forms. The first, using read–write inorganic crystals, can offer submillisecond access to large (Terabyte) blocks of data while still offering some degree of media removability. The second, using millimeter–thick disks of write–once media, offers high capacity in the conventional spinning–disk format.

Finally, spectrally–sensitive storage materials can be used to access yet another storage dimension beyond the three spatial dimensions: the spectral, or wavelength, dimension. By burning persistent spectral holes, these materials can store and retrieve data that is arranged either spatially or temporally (or even both). Because of their ability to perform Fourier transforms on input data, both holographic and spectrally–sensitive storage can also be applied towards data processing applications (correlation and pattern recognition, signal processing, associative and content–addressable memories, and even optical logic/optical computing).

The hurdles between current research and reliable, competitive products are numerous. All of these techniques are unattractive with current laser technology: each needs smaller, cheaper, and higher–power lasers and especially high–repetition rate, high–average–power, pulsed lasers for spinning disk systems. Holographic and spectrally–sensitive storage need single–spatial–mode lasers with high stability, and both would profit from the development of rapidly–tunable lasers in the visible.

Even more important than the laser source, these storage techniques live and die by the performance of the storage media. An interesting trend is observable in each of these disparate types of volumetric optical storage: each has started with materials that simply responded linearly to illumination, recognized the limitations that this imposed on volumetric selectivity (and non–volatile readout of read–write storage), and moved to find media which respond either nonlinearly or are gated in some way. With localized–bit storage, these are the two–photon absorption/fluorescence materials; with holographic storage, the gated, two–color photorefractives; with spectrally–sensitive storage, the photon–gated hole burning materials. The cost of using such a two–photon process is typically a reduction in sensitivity.

Then there are the supporting components, whether these are simply spindles and focus servos; or angle–deflectors, spatial light modulators, and CMOS detector arrays; or high–bandwidth modulators, acousto–optic deflectors, and robust, compact cryostats. In some cases, like the spatial light modulators and detector arrays, other commercial interests can drive much of the development; in others, the component development may need to be completed by those working on the volumetric storage technology that needs it.

The final pieces to the puzzle are the systems techniques, the tricks that finesse media and component problems, or the balancing of this tradeoff against that to arrive at a design point that satisifies all of the specifications. Sometimes, this is just simply recognizing what are deterministic variations rather than noise; sometimes, one recognizes the advantages of something the media “also” provides (such as the very low absorption that photon–gated materials can have once gating is completed).

The future of these volumetric storage technologies is hard to predict: some (or maybe even all!) of the storage methods described here may never progress past the research stage. While the demand for storage is almost certain to continue, the drive to research volumetric optical storage will depend not only on the progress made by its proponents, but also on the progress made in conventional storage and other prospective storage technologies. The vast unrealized potential of volumetric optical storage, the wide variety and maturity of already established techniques, and the almost universal recognition that “Tomorrow, I will need more storage” leads me to suspect that the work reviewed here will not be the final word.

REFERENCES

[1] Hecht, E. *Optics*. 2^{nd} edn., Addison–Wesley, **1987**.

[2] Mansuripur, M. *The physical principles of Magneto–optical recording*. Cambridge University Press, **1995**.

[3] Pu, A.; Psaltis, D. High–density recording in photopolymer–based holographic three–dimensional disks. Appl. Opt. **1996**, *35*(14), 2389–2398.

[4] Kawata, S. Photorefractive optics in three–dimensional digital memory. Proc. IEEE **1999**, *87*(12), 2009–2020.

[5] Watanabe, M.; Juodkazis, S.; Sun, H. B.; Matsuo, S.; Misawa, H. Two–photon readout of three–dimensional memory in silica. Appl. Phys. Lett. **2000**, *77*(1), 13–15.

[6] Steckman, G. J.; Pu, A.; Psaltis, D. Storage density of shift multiplexed holographic memory. Appl. Opt. **2001**, *40*(20), 3387–3394.

[7] Burr, G. W.; Jefferson, C. M.; Coufal, H.; Jurich, M.; Hoffnagle, J. A.; Macfarlane, R. M.; Shelby, R. M. Volume holographic data storage at areal density of 250 gigapixels/in^2. Opt. Lett. **2001**, *26*(7), 444–446.

[8] Imai, T.; Yagi, S.; Tate, A.; Kurokawa, T.; Tanabe, T.; Yamamoto, M.; Imamura, S., Noise analysis and reduction of waveguide holographic read–only memory. In *Annual Meeting of the Optical Society of America*, **2000** 59.

[9] Rosen, H. J.; Rubin, K. A.; Tang, W. C.; Imaino, W. I., Multilayer optical recording (MORE). In *Optical Data Storage 1995*, vol. 2514 of *Proceedings of the SPIE*, **1995** 14–19.

[10] Ecma–267 standard: 120mm dvd – read–only disk. http://www.ecma.ch, **1999**.

[11] Aldridge, K.; Matheney, P., Dvd in detail. Tech. rep., Cinram, **1999**, http://www.discmfg.com/index3.html.

[12] Milster, T. D.; Upton, R. S.; Luo, H. Objective lens design for multiple–layer optical data storage. Opt. Eng. **1999**, *38*(2), 295–301.

[13] Bruneau, J. M.; Bechevet, B.; Germain, C. Optical design for a double level rewritable phase change disc. Japanese Journal of Applied Physics Part 1 **1998**, *37*(4B), 2168–2175.

[14] Muramatsu, E.; Yamaguchi, A.; Horikawa, K.; Kato, M.; Taniguchi, S.; Jinno, S.; Yamaguchi, M.; Kudo, H.; Inoue, A. The new re–writable disc system for digital versatile disc. Japanese Journal of Applied Physics Part 1 **1998**, *37*(4B), 2257–2258.

[15] Satoh, I.; Ohara, S.; Akahira, N.; Takenaga, M. Key technology for high density rewritable DVD (DVD–RAM). IEEE Transactions On Magnetics **1998**, *34*(2), 337–342.

[16] ECMA–272 Standard: 120mm DVD Rewritable Disk (DVD–RAM). http://www.ecma.ch, **1999**.

[17] C3D Technology breakthrough: 10–layer 140GB discs due soon. DVD Intelligence, Vol3, n11–14, p1+, **2000**.

[18] C3D, White paper. Tech. rep., Constellation 3D, **2000**, http://www.c-3d.net/whitepaper.html.

[19] Dvornikov, A. S.; Malkin, J.; Rentzepis, P. M. Spectroscopy and kinetics of photochromic materials for 3D optical memory devices. Journal of Physical Chemistry **1994**, *98*(27), 6746–6752.

[20] Malkin, J.; Zelichenok, A.; Krongauz, V.; Dvornikov, A. S.; Rentzepis, P. M. Photochromism and kinetics of Naphthacenequinones. Journal of the American Chemical Society **1994**, *116*(3), 1101–1105.

[21] Akimov, D. A.; Zheltikov, A. M.; Koroteev, N. I.; Magnitskii, S. A.; Naumov, A. N.; Sidorov-Biryukov, D. A.; Sokolyuk, N. T.; Fedotov, A. B. Data reading in three–dimensional optical–memory devices based on photochromic materials with the use of laser–induced fluorescence and coherent four–wave mixing. Laser Physics **1997**, *7*(6), 1242–1252.

[22] Koroteev, N. I.; Magnitskii, S. A.; Shubin, V. V.; Sokolyuk, N. T. Photochemical and spectroscopic properties of naphthacenequinones as candidates for 3D optical data storage. Japanese Journal of Applied Physics Part 1 **1997**, *36*(1B), 424–425.

[23] Koroteev, N. I.; Krikunov, S. A.; Magnitskii, S. A.; Malakhov, D. V.; Shubin, V. V. Two–photon single–beam "bit–by–bit" writing and fluorescent "page–by–page" reading 2.5D femtosecond optical data storage system. Japanese Journal of Applied Physics Part 1 **1998**, *37*(4B), 2279–2280.

[24] Zheltikov, A. M.; Koroteev, N. I.; Magnitskii, S. A.; Naumov, A. N.; Sidorov-Biryukov, D. A.; Fedotov, A. B. Local nondestructive data reading in three–dimensional memory systems based on the optical Kerr effect. Quantum Electronics **1998**, *28*(11), 942–944.

[25] Koroteev, N. I.; Magnitskii, S. A.; Tarasishin, A. V.; Zheltikov, A. M. High–density three–dimensional optical data storage with photonic band–gap structures. Laser Physics **1999**, *9*(6), 1253–1259.

[26] Parthenopoulos, D. A.; Rentzepis, P. M. Three–dimensional optical storage memory. Science **1989**, *245*(0), 843–845.

[27] Parthenopoulos, D. A.; Rentzepis, P. M. Two–photon volume information storage in doped polymer systems. J. Appl. Phys. **1990**, *68*(11), 5814–5818.

[28] Hunter, S.; Kiamilev, F.; Esener, S.; Parthenopoulos, D. A.; Rentzepis, P. M. Potentials of two–photon based 3–D optical memories for high performance computing. Appl. Opt. **1990**, *29*(14), 2058–2066.

[29] Dvornikov, A. S.; Rentzepis, P. M. Processes and materials for two–photon volume optical memories. Opt. Mem. Neur. Net. **1994**, *3*(2), 75–86.

[30] Hunter, S.; Solomon, C.; Esener, S.; Ford, J. E.; Dvornikov, A. S.; Rentzepis, P. M. Three–dimensional optical image storage by two–photon recording. Opt. Mem. Neur. Net. **1994**, *3*(2), 151–167.

[31] Dvornikov, A. S.; Rentzepis, P. M. Accessing 3D memory information by means of nonlinear absorption. Opt. Commun. **1995**, *119*(0), 341–346.

[32] Bhawalkar, J. D.; Swiatkiewicz, J.; Pan, S. J.; Samarabandu, J. K.; Liou, W. S.; He, G. S.; Berezney, R.; Cheng, P. C.; Prasad, P. N. Three–dimensional laser scanning two–photon fluorescence confocal microscopy of polymer materials using a new, efficient upconverting fluorophore. Scanning **1996**, *18*(8), 562–566.

[33] Dvornikov, A. S.; Cokgor, I.; Wang, M.; McCormickJr., F. B.; Esener, S. C.; Rentzepis, P. M. Materials and systems for two photon 3–D ROM devices. IEEE Transactions on Components, Packaging, and Manufacturing Technology-Part A **1997**, *20*(2), 203–212.

[34] Wang, M. M.; Esener, S. C.; McCormick, F. B.; Cokgor, I.; Dvornikov, A. S.; Rentzepis, P. M. Experimental characterization of a two–photon memory. Opt. Lett. **1997**, *22*(8), 558–560.

[35] Hell, S. W.; Booth, M.; Wilms, S.; Schnetter, C. M.; Kirsch, A. K.; Arndt-Jovin, D. J.; Jovin, T. M. Two–photon near– and far–field fluorescence microscopy with continuous–wave excitation. Opt. Lett. **1998**, *23*(15), 1238–1240.

[36] Pavel, E.; Mihailescu, I. N.; Hening, A.; Vlad, V. I.; Tugulea, L.; Diamandescu, I.; Bibicu, I.; Chipara, M. Three–dimensional memory effect in fluorescent photosensitive glass activated by europium and cerium. Opt. Lett. **1998**, *23*(16), 1304–1306.

[37] Toriumi, A.; Kawata, S.; Gu, M. Reflection confocal microscope readout system for three–dimensional photochromic optical data storage. Opt. Lett. **1998**, *23*(24), 1924–1926.

[38] Day, D.; Gu, M. Use of two–photon excitation for erasable–rewritable three–dimensional bit optical data storage in a photorefractive polymer. Opt. Lett. **1999**, *24*(14), 948–950.

[39] Gu, M.; Day, D. Use of continuous–wave illumination for two–photon three–dimensional optical bit data storage in a photobleaching polymer. Opt. Lett. **1999**, *24*(5), 288–290.

[40] Pudavar, H. E.; Joshi, M. P.; Prasad, P. N.; Reinhardt, B. A. High–density three–dimensional optical data storage in a stacked compact disk format with two–photon writing and single photon readout. Appl. Phys. Lett. **1999**, *74*(9), 1338–1340.

[41] Watanabe, M.; Juodkazis, S.; Sun, H. B.; Matsuo, S.; Misawa, H.; Miwa, M.; Kaneko, R. Transmission and photoluminescence images of three–dimensional memory in vitreous silica. Appl. Phys. Lett. **1999**, *74*(26), 3957–3959.

[42] McCormick, F. B.; Zhang, H.; Dvomikov, A.; Walker, E.; Chapman, C.; Kim, N.; Costa, J.; Esener, S.; Rentzepis, P., Parallel access 3–D multilayer optical storage using 2–photon recording. In *Advanced Optical Data Storage: Materials, Systems, and Interfaces to Computers*, vol. 3802 of *Proceedings of the SPIE*, **1999** 173–182.

[43] Kawata, S.; Amistoso, J. O. Characterization of organic photochromic materials as 3–D optical data storage media. Molecular Crystals and Liquid Crystals **2000**, *344*(1), 23–30.

[44] Kawata, S.; Kawata, Y. Three–dimensional optical data storage using photochromic materials. Chemical Reviews **2000**, *100*(5), 1777–1788.

[45] Yamasaki, K.; Juodkazis, S.; Watanabe, M.; Sun, H. B.; Matsuo, S.; Misawa, H. Recording by microexplosion and two–photon reading of three–dimensional optical memory in polymethylmethacrylate films. Appl. Phys. Lett. **2000**, *76*(8), 1000–1002.

[46] Wang, M. M.; Esener, S. C. Three–dimensional holographic stamping of multilayer bit–oriented nonlinear optical media. Appl. Opt. **2000**, *39*(11), 1835–1841.

[47] Wang, M. M.; Esener, S. C. Three–dimensional optical data storage in fluorescent dye–doped photopolymer. Appl. Opt. **2000**, *39*(11), 1826–1834.

[48] Chinn, S. R.; Swanson, E. A. Multilayer optical storage by low–coherence reflectometry. Opt. Lett. **1996**, *21*(12), 899–901.

[49] Ho, H.-P.; Wu, S.-Y.; Chan, K.-S.; Pun, E. Y. B.; Shum, P. A multi–layered optical disc scheme for high density storage using transparent media. Japanese Journal of Applied Physics Part 2 **2000**, *39*(6), 597–600.

[50] Day, D.; Gu, M. Effects of refractive–index mismatch on three–dimensional optical data–storage density in a two–photon bleaching polymer. Appl. Opt. **1998**, *37*(26), 6299–6304.

[51] Suzuki, M. A.; Hashida, T.; Hibino, J.; Kishimoto, Y. Multiple optical memory using photochromic spiropyran aggregates. Molecular Crystals and Liquid Crystals **1994**, *246*, 389–396.

[52] Toriumi, A.; Herrmann, J. M.; Kawata, S. Nondestructive readout of a photochromic optical memory with a near–infrared differential phase–contrast microscope. Opt. Lett. **1997**, *22*(8), 555–557.

[53] Strickler, J. H.; Webb, W. W. Three–dimensional optical data storage in refractive media by two–photon point excitation. Opt. Lett. **1991**, *16*(22), 1780–1782.

[54] Strickler, J. H.; Webb, W. W. 3–D optical data storage by two–photon excitation. Advanced Materials **1993**, *5*(6), 479–481.

[55] Kawata, Y.; Tanaka, T.; Kawata, S. Randomly accessible, multilayered optical memory with a $Bi_{12}SiO_{20}$ crystal. Appl. Opt. **1996**, *35*(26), 5308–5311.

[56] Ueki, H.; Kawata, Y.; Kawata, S. Three–dimensional optical bit–memory recording and reading with a photorefractive crystal: analysis and experiment. Appl. Opt. **1996**, *35*(14), 2457–2465.

[57] Kawata, Y.; Ishitobi, H.; Kawata, S. Use of two–photon absorption in a photorefractive crvstal for three–dimensional optical memory. Opt. Lett. **1998**, *23*(10), 756–758.

[58] Gu, M. Confocal readout of three–dimensional data bits recorded by the photorefractive effect under single–photon and two–photon excitation. Proc. IEEE **1999**, *87*(12), 2021–2029.

[59] Hisaka, M.; Ishitobi, H.; Kawata, S. Optical recording of reversed domains in a Ce–doped SBN:75 crystal for bit–oriented three–dimensional optical memory. Journal of the Optical Society of America B-Optical Physics **2000**, *17*(3), 422–426.

[60] Glezer, E. N.; Milosavljevic, M.; Huang, L.; Finlay, R. J.; Her, T.-H.; Callan, J. P.; Mazur, E. Three–dimensional optical storage inside transparent materials. Opt. Lett. **1996**, *21*(24), 2023–2025.

[61] Glezer, E. N.; Mazur, E. Ultrafast–laser driven micro–explosions in transparent materials. Appl. Phys. Lett. **1997**, *71*(7), 882–884.

[62] Kondo, Y.; Suzuki, T.; Inouye, H.; Miura, K.; Mitsuyu, T.; Hirao, K. Three–dimensional microscopic crystallization in photosensitive glass by femtosecond laser pulses at nonresonant wavelength. Japanese Journal of Applied Physics Part 2 **1998**, *37*(1AB), L94–L96.

[63] Qiu, J. R.; Miura, K.; Hirao, K. Three–dimensional optical memory using glasses as a recording medium through a multi–photon absorption process. Japanese Journal of Applied Physics Part 1 **1998**, *37*(4B), 2263–2266.

[64] Watanabe, M.; Sun, H. B.; Juodkazis, S.; Takahashi, T.; Matsuo, S.; Suzuki, Y.; Nishii, J.; Misawa, H. Three–dimensional optical data storage in vitreous silica. Japanese Journal of Applied Physics Part 2 **1998**, *37*(12B), L1527–L1530.

[65] Kawata, Y.; Ueki, H.; Hashimoto, Y.; Kawata, S. 3–Dimensional optical memory with a photorefractive crystal. Appl. Opt. **1995**, *34*(20), 4105–4110.

[66] Tanaka, T.; Kawata, S. Comparison of recording densities in three–dimensional optical storage systems: Multilayered bit recording versus angularly multiplexed holographic recording. J. Opt. Soc. Amer. A **1996**, *13*(5), 935–943.

[67] Wilson, T.; Kawata, Y.; Kawata, S. Readout of three–dimensional optical memories. Opt. Lett. **1996**, *21*(13), 1003–1005.

[68] Ishikawa, M.; Kawata, Y.; Egami, C.; Sugihara, O.; Okamoto, N.; Tsuckimori, M.; Watanabe, O. Reflection–type confocal readout for multilayered optical memory. Opt. Lett. **1998**, *23*(22), 1781–1783.

[69] Nakamura, O.; Kawata, S. 3–dimensional transfer–function analysis of the tomographic capability of a confocal fluorescence microscope. J. Opt. Soc. Amer. A **1990**, *7*(3), 522–526.

[70] Kawata, Y.; Juikaitis, R.; Tanaka, T.; Wilson, T.; Kawata, S. Differential phase–contrast microscope with a split detector for the readout system of a multilayered optical memory. Appl. Opt. **1996**, *35*(14), 2466–2470.

[71] Fermann, M. E.; Hofer, M.; Haberl, F.; Schmidt, A. J.; Turi, L. Additive–pulse–compression mode–locking of a Neodymium fiber laser. Opt. Lett. **1991**, *16*(4), 244–246.

[72] Fermann, M. E.; Yang, L. M.; Stock, M. L.; Andrejco, M. J. Environmentally stable Kerr–type mode–locked Erbium fiber laser producing 360–fs pulses. Opt. Lett. **1994**, *19*(1), 43–45.

[73] Yamada, E.; Yoshida, E.; Kitoh, T.; Nakazawa, M. Generation of terabit per second optical–data pulse–train. Electronics Letters **1995**, *31*(16), 1342–1344.

[74] Hansen, P. B.; Raybon, G.; Koren, U.; Miller, B. I.; Young, M. G.; Newkirk, M. A.; Chien, M. D.; Tell, B.; Burrus, C. A. 2–cm long monolithic multisection laser for active modelocking at 2.2 GHz. Electronics Letters **1993**, *29*(9), 739–741.

[75] Arahira, S.; Ogawa, Y. Synchronous mode–locking in passively mode–locked semiconductor laser diodes using optical short pulses repeated at subharmonics of the cavity round–trip frequency. IEEE Photonics Technology Letters **1996**, *8*(2), 191–193.

[76] Olson, B. H.; Paturi, R.; Esener, S. C. Biorthogonally accessed three–dimensional two–photon memory for relational database operations. Appl. Opt. **1997**, *36*(17), 3877–3888.

[77] Marhic, M. E. Storage limit of two–photon–based three–dimensional memories with parallel access. Opt. Lett. **1991**, *16*(16), 1272–1273.

[78] Birge, R. R. Protein–based optical computing and memories. Computer **1992**, *0*(0), 56–67.

[79] Birge, R. R. Protein–based computers. Scientific American **1995**, *0*(0), 90–95.

[80] Birge, R. R.; Gillespie, N. B.; Izaguirre, E. W.; Kusnetzow, A.; Lawrence, A. F.; Singh, D.; Song, Q. W.; Schmidt, E.; Stuart, J. A.; Seetharaman, S.; Wise, K. J. Biomolecular electronics: Protein–based associative processors and volumetric memories. Journal of Physical Chemistry B **1999**, *103*(49), 10746–10766.

[81] Coufal, H. J.; Psaltis, D.; Sincerbox, G., eds. *Holographic Data Storage*. Springer–Verlag, **2000**.

[82] Colburn, W. S.; Haines, K. A. Volume hologram formation in photopolymer materials. Appl. Opt. **1971**, *10*(7), 1636–1641.

[83] Ashkin, A.; Boyd, G. D.; Dziedzic, J. M.; Smith, R. G.; Ballman, A. A.; Levinstein, J. J.; Nassau, K. Optically–induced refractive index homogeneities in $LiNbO_3$ and $LiTaO_3$. Appl. Phys. Lett. **1966**, *9*(1), 72–74.

[84] Collier, R. J.; Burckhardt, C. B.; Lin, L. H. *Optical holography*. Academic Press, San Diego, **1971**.

[85] Goodman, J. W. *Introduction to Fourier Optics*. 2nd edn., McGraw–Hill, **1996**.

[86] van Heerden, P. J. Theory of optical information storage in solids. Appl. Opt. **1963**, *2*(4), 393–401.

[87] van Heerden, P. J. A new optical method of storing and retrieving information. Appl. Opt. **1963**, *2*(4), 387–392.

[88] Leith, E. N.; Kozma, A.; Upatnieks, J.; Marks, J.; Massey, N. Holographic data storage in three–dimensional media. Appl. Opt. **1966**, *5*(8), 1303–1311.

[89] Psaltis, D.; Mok, F. Holographic memories. Scientific American **1995**, *273*(5), 70–76.

[90] Heanue, J. F.; Bashaw, M. C.; Hesselink, L. Volume holographic storage and retrieval of digital data. Science **1994**, *265*(5173), 749–752.

[91] Hong, J. H.; McMichael, I.; Chang, T. Y.; Christian, W.; Paek, E. G. Volume holographic memory systems: techniques and architectures. Opt. Eng. **1995**, *34*(8), 2193–2203.

[92] Psaltis, D.; Burr, G. W. Holographic data storage. Computer **1998**, *31*(2), 52.

[93] Ashley, J.; Bernal, M.-P.; Burr, G. W.; Coufal, H.; Guenther, H.; Hoffnagle, J. A.; Jefferson, C. M.; Marcus, B.; Macfarlane, R. M.; Shelby, R. M.; Sincerbox, G. T. Holographic data storage. IBM J. Res. Dev. **2000**, *44*(3), 341–368.

[94] Amodei, J. J.; Staebler, D. L. Holographic pattern fixing in electro–optic crystals. Appl. Phys. Lett. **1971**, *18*(12), 540–542.

[95] Stewart, W. C.; Mezrich, R. S.; Cosentin, L. S.; Nagle, E. M.; Wendt, F. S.; Lohman, R. D. Experimental read–write holographic memory. RCA Review **1973**, *34*(1), 3–44.

[96] D'Auria, L.; Huignard, J. P.; Slezak, C.; Spitz, E. Experimental holographic read–write memory using 3–D storage. Appl. Opt. **1974**, *13*(4), 808–818.

[97] Huignard, J. P.; Herriau, J. P.; Micheron, F. Coherent selective erasure of superimposed volume holograms in $LiNbO_3$. Appl. Phys. Lett. **1975**, *26*(5), 256–258.

[98] Staebler, D. L.; Burke, W. J.; Phillips, W.; Amodei, J. J. Multiple storage and erasure of fixed holograms in Fe–doped $LiNbO_3$. Appl. Phys. Lett. **1975**, *26*(4), 182–184.

[99] Bartolini, R. A.; Bloom, A.; Escher, J. S. Multiple storage of holograms in an organic medium. Appl. Phys. Lett. **1976**, *28*(9), 506–507.

[100] Mok, F. H.; Tackitt, M. C.; Stoll, H. M. Storage of 500 high–resolution holograms in a $LiNbO_3$ crystal. Opt. Lett. **1991**, *16*(8), 605–607.

[101] Mok, F. H. Angle–multiplexed storage of 5000 holograms in lithium niobate. Opt. Lett. **1993**, *18*(11), 915–917.

[102] Tao, S.; Selviah, D. R.; Midwinter, J. E. Spatioangular multiplexed storage of 750 holograms in an Fe:$LiNbO_3$ crystal. Opt. Lett. **1993**, *18*(11), 912–914.

[103] An, X.; Psaltis, D. Experimental characterization of an angle–multiplexed holographic memory. Opt. Lett. **1995**, *20*(18), 1913–1915.

[104] Bernal, M. P.; Coufal, H.; Grygier, R. K.; Hoffnagle, J. A.; Jefferson, C. M.; Macfarlane, R. M.; Shelby, R. M.; Sincerbox, G. T.; Wimmer, P.; Wittmann, G. A precision tester for studies of holographic optical storage materials and recording physics. Appl. Opt. **1996**, *35*(14), 2360–2374.

[105] McMichael, I.; Christian, W.; Pletcher, D.; Chang, T. Y.; Hong, J. H. Compact holographic storage demonstrator with rapid access. Appl. Opt. **1996**, *35*(14), 2375–2379.

[106] Drolet, J. J. P.; Chuang, E.; Barbastathis, G.; Psaltis, D. Compact, integrated dynamic holographic memory with refreshed holograms. Opt. Lett. **1997**, *22*(8), 552–554.

[107] Chuang, E.; Psaltis, D. Storage of 1000 holograms with use of a dual–wavelength method. Appl. Opt. **1997**, *36*(32), 8445–8454.

[108] Dhar, L.; Curtis, K.; Tackitt, M.; Schilling, M.; Campbell, S.; Wilson, W.; Hill, A.; Boyd, C.; Levinos, N.; Harris, A. Holographic storage of multiple high–capacity digital data pages in thick photopolymer systems. Opt. Lett. **1998**, *23*(21), 1710–1712.

[109] Chuang, E.; Liu, W. H.; Drolet, J. J. P.; Psaltis, D. Holographic random access memory (HRAM). Proc. IEEE **1999**, *87*(11), 1931–1940.

[110] Ma, J. A.; Chang, T.; Choi, S.; Hong, J. Ruggedized digital holographic data storage with fast access. Optical and Quantum Electronics **2000**, *32*(3), 383–392.

[111] Wilson, W. L.; Curtis, K.; Tackitt, M.; Hill, A.; Hale, A.; Schilling, M.; Boyd, C.; Campbell, S.; Dhar, L.; Harris, A. High density, high performance optical data storage via volume holography: Viability at last? Optical and Quantum Electronics **2000**, *32*(3), 393–404.

[112] Zhou, G.; Psaltis, D.; Mok, F. Holographic read–only memory. Optical and Quantum Electronics **2000**, *32*(3), 405–417.

[113] Orlov, S. S. Volume holographic data storage. Communications of the ACM **2000**, *43*(11), 46–54.

[114] Martynov, Y. V.; Wierenga, H. A. Migration path of optical storage drives and media. Journal of Information Storage and Processing Systems **2000**, *2*(1), 93–100.

[115] Fukui, M.; Kitayama, K. Real–time restoration method for image transmission in a multimode optical fiber. Opt. Lett. **1990**, *15*(17), 977–979.

[116] Ito, F.; Kitayama, K. I.; Oguri, H. Compensation of fiber holographic image distortion caused by intrasignal photorefractive coupling by using a phase–conjugate mirror. Opt. Lett. **1992**, *17*(3), 215–217.

[117] Aharoni, A.; Bashaw, M. C.; Hesselink, L. Distortion–free multiplexed holography in striated photorefractive media. Appl. Opt. **1993**, *32*(11), 1973–1982.

[118] Campbell, S.; Yeh, P. C.; Gu, C.; He, Q. B. Fidelity of image–restoration by partial phase–conjugation through multimode fibers. Opt. Commun. **1995**, *114*(1-2), 50–56.

[119] Kitayama, K.; Ito, F. Holographic memory using long photorefractive fiber array. Optical Materials **1995**, *4*(2-3), 392–398.

[120] Zhao, F.; Sayano, K. Compact read–only memory with lensless phase–conjugate holograms. Opt. Lett. **1996**, *21*(16), 1295–1297.

[121] Burr, G. W.; Leyva, I. Multiplexed phase–conjugate holographic data storage with a buffer hologram. Opt. Lett. **2000**, *25*(7), 499–501.

[122] Psaltis, D.; Brady, D.; Wagner, K. Adaptive optical networks using photorefractive crystals. Appl. Opt. **1988**, *27*(9), 1752–1759.

[123] Henshaw, P. D.; Lis, S. A., Content addressable optical data storage system. U. S. Patent #5,319,629, **1994**.

[124] Goertzen, B. J.; Mitkas, P. A. Volume holographic storage for large relational databases. Opt. Eng. **1995**, *35*(7), 1847–1853.

[125] Burr, G. W.; Kobras, S.; Hanssen, H.; Coufal, H. Content–addressable data storage by use of volume holograms. Appl. Opt. **1999**, *38*(32), 6779–6784.

[126] Betzos, G. A.; Laisne, A.; Mitkas, P. A. Improved associative recall of binary data in volume holographic memories. Opt. Commun. **1999**, *171*(1-3), 37–44.

[127] Rakuljic, G. A.; Leyva, V.; Yariv, A. Optical data storage by using orthogonal wavelength–multiplexed volume holograms. Opt. Lett. **1992**, *17*(20), 1471–1473.

[128] Yin, S.; Zhou, H.; Zhao, F.; Wen, M.; Yang, Z.; Zhang, J.; Yu, F. T. S. Wavelength multiplexed holographic storage in a sensitive photorefractive crystal using a visible–light tunable diode laser. Opt. Commun. **1993**, *101*, 317–321.

[129] Ford, J. E.; Fainman, Y.; Lee, S. H. Array interconnection by phase–coded optical correlation. Opt. Lett. **1990**, *15*(19), 1088–1090.

[130] Denz, C.; Pauliat, G.; Roosen, G.; Tschudi, T. Volume hologram multiplexing using a deterministic phase encoding method. Opt. Commun. **1991**, *85*, 171–176.

[131] Denz, C.; Pauliat, G.; Roosen, G.; Tschudi, T. Potentialities and limitations of hologram multiplexing by using the phase–encoding technique. Appl. Opt. **1992**, *31*(26), 5700–5705.

[132] Burr, G. W., *Volume holographic storage using the 90° geometry*. Ph.D. thesis, California Institute of Technology, Pasadena, Calif., **1996**.

[133] An, X.; Psaltis, D.; Burr, G. W. Thermal fixing of 10,000 holograms in $LiNbO_3$:Fe. Appl. Opt. **1999**, *38*(2), 386–393.

[134] Wang, X.; Wilson, D.; Muller, R.; Maker, P.; Psaltis, D. Liquid–crystal blazed–grating beam deflector. Appl. Opt. **2000**, *39*(35), 6545–6555.

[135] Burr, G. W.; Ashley, J.; Coufal, H.; Grygier, R. K.; Hoffnagle, J. A.; Jefferson, C. M.; Marcus, B. Modulation coding for pixel–matched holographic data storage. Opt. Lett. **1997**, *22*(9), 639–641.

[136] Shelby, R. M.; Hoffnagle, J. A.; Burr, G. W.; Jefferson, C. M.; Bernal, M.-P.; Coufal, H.; Grygier, R. K.; Gunther, H.; Macfarlane, R. M.; Sincerbox, G. T. Pixel–matched holographic data storage with megabit pages. Opt. Lett. **1997**, *22*(19), 1509–1511.

[137] Curtis, K.; Pu, A.; Psaltis, D. Method for holographic storage using peristrophic multiplexing. Opt. Lett. **1994**, *19*(13), 993–994.

[138] Li, H. S.; Psaltis, D. Three–dimensional holographic optical disks. Appl. Opt. **1994**, *33*(17), 3764–3774.

[139] Psaltis, D.; Levene, M.; Pu, A.; Barbastathis, G.; Curtis, K. Holographic storage using shift multiplexing. Opt. Lett. **1995**, *20*(7), 782–784.

[140] Psaltis, D.; Pu, A. Holographic 3–D disks. Optoelectronics-Devices and Technologies **1995**, *10*(3), 333–342.

[141] Barbastathis, G.; Levene, M.; Psaltis, D. Shift multiplexing with spherical reference waves. Appl. Opt. **1996**, *35*(14), 2403–2417.

[142] Burr, G. W.; Mok, F. H.; Psaltis, D. Angle and space multiplexed holographic storage using the 90–degrees geometry. Opt. Commun. **1995**, *117*(1-2), 49–55.

[143] Booth, B. L. Photopolymer material for holography. Appl. Opt. **1975**, *14*(3), 593–601.

[144] Ingwall, R. T.; Fielding, H. L. Hologram recording with a new photopolymer system. Opt. Eng. **1985**, *24*(5), 808–811.

[145] Ingwall, R. T.; Troll, M. Mechanism of hologram formation in DMP–128 photopolymer. Opt. Eng. **1989**, *28*(6), 586–591.

[146] Curtis, K.; Psaltis, D. Recording of multiple holograms in photopolymer films. Appl. Opt. **1992**, *31*(35), 7425–7428.

[147] Gallo, J. T.; Verber, C. M. Model for the effects of material shrinkage on volume holograms. Appl. Opt. **1994**, *33*(29), 6797–6804.

[148] Rhee, U.; Caulfield, H. J.; Vikram, C. S.; Shamir, J. Dynamics of hologram recording in DuPont photopolymer. Appl. Opt. **1995**, *34*(5), 846–853.

[149] Weitzel, K. T.; Wild, U. P.; Mikhailov, V. N.; Krylov, V. N. Hologram recording in DuPont photopolymer films by use of pulse exposure. Opt. Lett. **1997**, *22*(24), 1899–1901.

[150] Dhar, L.; Schnoes, M. G.; Wysocki, T. L.; Bair, H.; Schilling, M.; Boyd, C. Temperature–induced changes in photopolymer volume holograms. Appl. Phys. Lett. **1998**, *73*(10), 1337–1339.

[151] Mikhailov, V. N.; Krylov, V. N.; Vaitsel, K. T.; Wild, U. P. Recording of pulsed holograms in photopolymer materials. Optics and Spectroscopy **1998**, *84*(4), 589–596.

[152] Bieringer, T.; Wuttke, R.; Haarer, D. Relaxation of holographic gratings in liquid–crystalline side–chain polymers with azo chromophores. Macromolecular Chemistry and Physics **1995**, *196*(5), 1375–1390.

[153] Zilker, S. J.; Bieringer, T.; Haarer, D.; Stein, R. S.; van Egmond, J. W.; Kostromine, S. G. Holographic data storage in amorphous polymers. Advanced Materials **1998**, *10*(11), 855.

[154] Eickmans, J.; Bieringer, T.; Kostromine, S.; Berneth, H.; Thoma, R. Photoaddressable polymers: a new class of materials for optical data storage and holographic memories. Japanese Journal of Applied Physics Part 1 **1999**, *38*(3B), 1835–1836.

[155] Theissen, U.; Zilker, S. J.; Pfeuffer, T.; Strohriegl, P. Photopolymerizable cholesteric liquid crystals – new materials for holographic applications. Advanced Materials **2000**, *12*(22), 1698.

[156] Steckman, G. J.; Solomatine, I.; Zhou, G.; Psaltis, D. Characterization of phenanthrenequinone–doped poly(methyl methacrylate) for holographic memory. Opt. Lett. **1998**, *23*(16), 1310–1312.

[157] Lin, S. H.; Hsu, K. Y.; Chen, W. Z.; Whang, W. T. Phenanthrenequinone–doped poly(methyl methacrylate) photopolymer bulk for volume holographic data storage. Opt. Lett. **2000**, *25*(7), 451–453.

[158] Popov, A.; Novikov, I.; Lapushka, K.; Zyuzin, I.; Ponosov, Y.; Ashcheulov, Y.; Veniaminov, A. Spectrally selective holographic optical elements based on a thick polymer medium with diffusional amplification. Journal of Optics A-Pure and Applied Optics **2000**, *2*(5), 494–499.

[159] Steckman, G. J.; Shelkovnikov, V.; Berezhnaya, V.; Gerasimova, T.; Solomatine, I.; Psaltis, D. Holographic recording in a photopolymer by optically induced detachment of chromophores. Opt. Lett. **2000**, *25*(9), 607–609.

[160] Schnoes, M. G.; Dhar, L.; Schilling, M. L.; Patel, S. S.; Wiltzius, P. Photopolymer–filled nanoporous glass as a dimensionally stable holographic recording medium. Opt. Lett. **1999**, *24*(10), 658–660.

[161] Shelby, R. M.; Waldman, D. A.; Ingwall, R. T. Distortions in pixel–matched holographic data storage due to lateral dimensional change of photopolymer storage media. Opt. Lett. **2000**, *25*(10), 713–715.

[162] Burr, G. W.; Weiss, T. Compensation for pixel misregistration in volume holographic data storage. Opt. Lett. **2001**, *26*(8), 542–544.

[163] Hoffnagle, J. A.; Jefferson, C. M. Design and performance of a refractive optical system that converts a Gaussian to a flattop beam. Appl. Opt. **2000**, *39*(30), 5488–5499.

[164] Birabassov, R.; Landraud, N.; Galstyan, T. V.; Ritcey, A.; Bazuin, C. G.; Rahem, T. Thick dye–doped poly(methyl methacrylate) films for real–time holography. Appl. Opt. **1998**, *37*(35), 8264–8269.

[165] Jang, J. S.; Shin, D. H.; Park, Y. S. Holographic data storage by combined use of peristrophic, angular, and spatial multiplexing. Opt. Eng. **2000**, *39*(11), 2975–2981.

[166] Sun, C.-C.; Su, W.-C.; Lin, Y.-N.; Yang, Y. O.; Yeh, S.-P.; Wang, B. Three dimensional shifting sensitivity of a volume hologram with spherical reference waves. Opt. Mem. Neur. Net. **1999**, *8*(4), 229–236.

[167] Markov, V. B. Spatial–angular selectivity of 3–D speckle–wave holograms and information storage. Journal of Imaging Science and Technology **1997**, *41*(4), 383–388.

[168] Markov, V. B.; Denisyuk, Y. N.; Amezquita, R. 3–D speckle–shift hologram and its storage capacity. Opt. Mem. Neur. Net. **1997**, *6*(2), 91–98.

[169] Kang, Y. H.; Kim, K. H.; Lee, B. Angular and speckle multiplexing of photorefractive holograms by use of fiber speckle patterns. Appl. Opt. **1998**, *37*(29), 6969–6972.

[170] Burke, W. J.; Staebler, D. L.; Phillips, W.; Alphonse, G. A. Volume phase holographic storage in ferroelectric crystals. Opt. Eng. **1978**, *17*(4), 308–316.

[171] Glass, A. M. The photorefractive effect. Opt. Eng. **1978**, *17*(5), 470–479.

[172] Gunter, P. Holography, coherent light amplification and optical phase conjugation with photorefractive materials. Physics Reports **1982**, *4*, 199–299.

[173] Gunter, P.; Huignard, J.-P., eds. *Topics in Applied Physics—Vol. 61: Photorefractive Materials and Their Applications I—Fundamental Phenomena*. Springer–Verlag, **1988**.

[174] Yeh, P.; Chiou, A. E.; Hong, J.; Beckwith, P.; Chang, T.; Khoshnevisan, M. Photorefractive nonlinear optics and optical computing. Opt. Eng. **1989**, *28*(4), 328–343.

[175] Chen, F. S.; LaMacchia, J. T.; Fraser, D. B. Holographic storage in lithium niobate. Appl. Phys. Lett. **1968**, *13*(7), 223–225.

[176] Staebler, D. L.; Phillips, W. Fe–doped $LiNbO_3$ for read–write applications. Appl. Opt. **1974**, *13*(4), 788–794.

[177] Thaxter, J. B. Electrical control of holographic storage in strontium–barium niobate. Appl. Phys. Lett. **1969**, *15*(7), 210.

[178] Micheron, F.; Bismuth, G. Electrical control of fixation and erasure of holographic patterns in ferroelectric materials. Appl. Phys. Lett. **1972**, *20*(2), 79.

[179] Ma, J. A.; Chang, T.; Hong, J.; Neurgaonkar, R.; Barbastathis, G.; Psaltis, D. Electrical fixing of 1000 angle–multiplexed holograms in SBN:75. Opt. Lett. **1997**, *22*(14), 1116–1118.

[180] Townsend, R. L.; Lamacchi, J. T. Optically induced refractive index changes in $BaTiO_3$. J. Appl. Phys. **1970**, *41*(13), 5188.

[181] Feinberg, J.; Heiman, D.; Tanguay, A. R.; Hellwarth, R. W. Photorefractive effects and light–induced charge migration in barium–titanate. J. Appl. Phys. **1980**, *51*(3), 1297–1305.

[182] Kratzig, E.; Welz, F.; Orlowski, R.; Doormann, V.; Rosenkranz, M. Holographic storage properties of $BaTiO_3$. Solid State Communications **1980**, *34*(10), 817–819.

[183] Brady, D.; Hsu, K.; Psaltis, D. Periodically refreshed multiply exposed photorefractive holograms. Opt. Lett. **1990**, *15*(14), 817–819.

[184] Qiao, Y.; Psaltis, D.; Gu, C.; Hong, J.; Yeh, P.; Neurgaonkar, R. R. Phase–locked sustainment of photorefractive holograms using phase conjugation. J. Appl. Phys. **1991**, *70*(8), 4646–4648.

[185] Boj, S.; Pauliat, G.; Roosen, G. Dynamic holographic memory showing readout, refreshing, and updating capabilities. Opt. Lett. **1992**, *17*(6), 438–440.

[186] Piazzolla, S.; Jenkins, B. K.; Tanguay, A. R. Single–step copying process for multiplexed volume holograms. Opt. Lett. **1992**, *17*(9), 676–678.

[187] Qiao, Y.; Psaltis, D. Sampled dynamic holographic memory. Opt. Lett. **1992**, *17*(19), 1376–1378.

[188] Yeh, P.; Gu, C.; Cheng, C.; Hsu, K. Y. Optical restoration of photorefractive holograms. Applied Physics B **1995**, *61*(5), 511–514.

[189] Dellwig, T.; Denz, C.; Rauch, T.; Tschudi, T. Coherent refreshment and updating for dynamic photorefractive optical memories using phase conjugation. Opt. Commun. **1995**, *119*, 333–340.

[190] Esselbach, M.; Cedilnik, G.; Kiessling, A.; Kowarschik, R. Optical information storage using refresh via phase conjugation. Optics and Laser Technology **1999**, *31*(8), 579–582.

[191] Amodei, J. J.; Phillips, W.; Staebler, D. L. Improved electrooptic materials and fixing techniques for holographic recording. Appl. Opt. **1972**, *11*(2), 390–396.

[192] Meyer, W.; Wurfel, P.; Munser, R.; Mullervogt, G. Kinetics of fixation of phase holograms in $LiNbO_3$. Physica Status Solidi A **1979**, *53*(1), 171–180.

[193] Vormann, H.; Weber, G.; Kapphan, S.; Kratzig, E. Hydrogen as origin of thermal fixing in $LiNbO_3$:Fe. Solid State Communications **1981**, *40*, 543–545.

[194] Carrascosa, M.; Agullo-Lopez, F. Theoretical modeling of the fixing and developing of holographic gratings in $LiNbO_3$. J. Opt. Soc. Amer. B **1990**, *7*(12), 2317–2322.

[195] Yariv, A.; Orlov, S.; Rakuljic, G.; Leyva, V. Holographic fixing, readout, and storage dynamics in photorefractive materials. Opt. Lett. **1995**, *20*(11), 1334–1336.

[196] Buse, K.; Breer, S.; Peithmann, K.; Kapphan, S.; Gao, M.; Kratzig, E. Origin of thermal fixing in photorefractive lithium niobate crystals. Phys. Rev. B **1997**, *56*(3), 1225–1235.

[197] Rakuljic, G. A. Prescription for long–lifetime, high–diffraction–efficiency fixed holograms in Fe–doped $LiNbO_3$. Opt. Lett. **1997**, *22*(11), 825–827.

[198] Arizmendi, L.; de Miguel–Sanz, E. M.; Carrascosa, M. Lifetimes of thermally fixed holograms in $LiNbO_3$:Fe crystals. Opt. Lett. **1998**, *23*(12), 960–962.

[199] Cudney, R. S.; Fousek, J.; Zgonik, M.; Gunter, P.; Garrett, M. H.; Rytz, D. Enhancement of the amplitude and lifetime of photoinduced space–charge fields in multidomain ferroelectric–crystals. Phys. Rev. Lett. **1994**, *72*(24), 3883–3886.

[200] Ma, J.; Chang, T. Y.; Hong, J. H.; Neurgaonkar, R. R. Enhancement of multiplexed holograms in cerium–doped $Sr_{0.75}Ba_{0.25}Nb_2O_6$. Phys. Rev. Lett. **1997**, *78*(15), 2960–2963.

[201] Von der Linde, D.; Glass, A. M.; Rodgers, K. F. Multiphoton photorefractive processes for optical storage in $LiNbO_3$. Appl. Phys. Lett. **1974**, *25*(3), 155–157.

[202] Von der Linde, D.; Glass, A. M.; Rodgers, K. F. Optical storage using refractive–index changes induced by 2–step excitation. J. Appl. Phys. **1976**, *47*(1), 217–220.

[203] Vormann, H.; Kratzig, E. Two step excitation in $LiTaO_3$:Fe for optical data storage. Solid State Communications **1984**, *49*(9), 843–847.

[204] Jermann, F.; Otten, J. Light–induced charge transport in $LiNbO_3$:Fe at high light intensities. J. Opt. Soc. Amer. B **1993**, *10*(11), 2085–2092.

[205] Jermann, F.; Simon, M.; Kratzig, E. Photorefractive properties of congruent and stoichiometric lithium niobate at high light intensities. J. Opt. Soc. Amer. B **1995**, *12*(11), 2066–2070.

[206] Guenther, H.; Wittmann, G.; Macfarlane, R. M.; Neurgaonkar, R. R. Intensity dependence and white–light gating of two–color photorefractive gratings in $LiNbO_3$. Opt. Lett. **1997**, *22*(17), 1305–1307.

[207] Buse, K.; Adibi, A.; Psaltis, D. Non–volatile holographic storage in doubly doped lithium niobate crystals. Nature **1998**, *393*(6686), 665–668.

[208] Guenther, H.; Macfarlane, R.; Furukawa, Y.; Kitamura, K.; Neurgaonkar, R. Two–color holography in reduced near–stoichiometric lithium niobate. Appl. Opt. **1998**, *37*(32), 7611–7623.

[209] Hesselink, L.; Orlov, S. S.; Liu, A.; Akella, A.; Lande, D.; Neurgaonkar, R. R. Photorefractive materials for nonvolatile volume holographic data storage. Science **1998**, *282*(5391), 1089–1094.

[210] Liu, Y. W.; Liu, L. R.; Zhou, C. H. Prescription for optimizing holograms in $LiNbO_3$:Fe:Mn. Opt. Lett. **2000**, *25*(8), 551–553.

[211] Ducharme, S.; Scott, J. C.; Twieg, R. J.; Moerner, W. E. Observation of the photorefractive effect in a polymer. Phys. Rev. Lett. **1991**, *66*(14), 1846–1849.

[212] Silence, S. M.; Walsh, C. A.; Scott, J. C.; Matray, T. J.; Twieg, R. J.; Hache, F.; Bjorklund, G. C.; Moerner, W. E. Subsecond grating growth in a photorefractive polymer. Opt. Lett. **1992**, *17*(16), 1107–1109.

[213] Meerholz, K.; Volodin, B. L.; Sandalphon; Kippelen, B.; Peyghambarian, N. A photorefractive polymer with high optical gain and diffraction efficiency near 100%. Nature **1994**, *371*, 497–500.

[214] Moerner, W. E.; Silence, S. M. Polymeric photorefractive materials. Chemical Reviews **1994**, *94*(1), 127–155.

[215] Lundquist, P. M.; Wortmann, R.; Geletneky, C.; Twieg, R. J.; Jurich, M.; Lee, V. Y.; Moylan, C. R.; Burland, D. M. Organic glasses: a new class of photorefractive materials. Science **1996**, *274*(5290), 1182–1185.

[216] Zhang, Y.; Burzynski, R.; Ghosal, S.; Casstevens, M. K. Photorefractive polymers and composites. Advanced Materials **1996**, *8*(2), 111–125.

[217] Meerholz, K. Amorphous plastics pave the way to widespread holographic applications. Angewandte Chemie-International Edition in English **1997**, *36*(9), 945–948.

[218] Moerner, W. E.; Grunnet-Jepsen, A.; Thompson, C. L. Photorefractive polymers. Annual Review of Materials Science **1997**, *27*, 585–623.

[219] Oesterhelt, D.; Brauchle, C.; Hampp, N. Bacteriorhodopsin – a biological–material for information–processing. Quarterly Reviews of Biophysics **1991**, *24*(4), 425–478.

[220] Downie, J. D. Real–time holographic image correction using bacteriorhodopsin. Appl. Opt. **1994**, *33*(20), 4353–4357.

[221] Zhang, Y. H.; Song, Q. W.; Tseronis, C.; Birge, R. R. Real–time holographic imaging with a bacteriorhodopsin film. Opt. Lett. **1995**, *20*(23), 2429–2431.

[222] Downie, J. D.; Smithey, D. T. Measurements of holographic properties of bacteriorhodopsin films. Appl. Opt. **1996**, *35*(29), 5780–5789.

[223] Downie, J. D.; Timucin, D.; Smithey, D. T.; Crew, M. Long holographic lifetimes in bacteriorhodopsin films. Opt. Lett. **1998**, *23*(9), 730–732.

[224] Hampp, N. Bacteriorhodopsin as a photochromic retinal protein for optical memories. Chemical Reviews **2000**, *100*(5), 1755–1776.

[225] Linke, R. A.; Thio, T.; Chadi, J. D.; Devlin, G. E. Diffraction from optically written persistent plasma gratings in doped compound semiconductors. Appl. Phys. Lett. **1994**, *65*(1), 16–18.

[226] Macdonald, R. L.; Linke, R. A.; Chadi, J. D.; Thio, T.; Devlin, G. E. Thick plasma gratings using a local photorefractive effect in CdZnTe–In. Opt. Lett. **1994**, *19*(24), 2131–2133.

[227] Redmond, I. R.; Linke, R. A.; Chuang, E.; Psaltis, D. Holographic data storage in a DX–center material. Opt. Lett. **1997**, *22*(15), 1189–1191.

[228] Linke, R. A.; Redmond, I.; Thio, T.; Chadi, D. J. Holographic storage media based on optically active bistable defects. J. Appl. Phys. **1998**, *83*(2), 661–673.

[229] Ashley, J. J.; Marcus, B. H. Two–dimensional low–pass filtering codes. IEEE Transactions On Communications **1998**, *46*(6), 724–727.

[230] Chou, W. C.; Neifeld, M. A. Interleaving and error correction in volume holographic memory systems. Appl. Opt. **1998**, *37*(29), 6951–6968.

[231] Dhar, L.; Hale, A.; Katz, H. E.; Schilling, M. L.; Schnoes, M. G.; Schilling, F. C. Recording media that exhibit high dynamic range for digital holographic data storage. Opt. Lett. **1999**, *24*(7), 487–489.

[232] Wullert, J. R.; Delfyett, P. J. Multiwavelength, multilevel optical storage using dielectric mirrors. IEEE Photonics Technology Letters **1994**, *6*(9), 1133–1135.

[233] Homan, S.; Willner, A. E., High–capacity optical storage using multiple wavelengths, multiple layers and volume holograms. In *Optical Data Storage '95*, vol. 2514 of *Proceedings of the SPIE*, **1995** 184–190.

[234] Eichler, H. J.; Kuemmel, P.; Orlic, S.; Wappelt, A. High–density disk storage by multiplexed microholograms. IEEE Journal of Selected Topics in Quantum Electronics **1998**, *4*(5), 840–848.

[235] Labeyrie, A.; Huignard, J. P.; Loiseaux, B. Optical data storage in microfibers. Opt. Lett. **1998**, *23*(4), 301–303.

[236] Chi, C. J.; Steckl, A. J. Digital thin–film color optical memory. Appl. Phys. Lett. **2001**, *78*(2), 255–257.

[237] Stroke, G. W.; Labeyrie, A. E. White–light reconstruction of holographic images using Lippmann–Bragg diffraction effect. Physics Letters **1966**, *20*(4), 368.

[238] Morinaka, A.; Oikawa, S.; Yamazaki, H. Optical–recording media with thermal coloration. Appl. Phys. Lett. **1983**, *43*(6), 524–526.

[239] Caine, E. J.; Miller, S. D. Optical data storage in LiF using electron beam encoding. Journal of Vacuum Science & Technology B **1998**, *16*(6), 3232–3236.

[240] Baba, K.; Yamada, R.; Nakao, S.; Miyagi, M. Multifrequency 3–Dimensional optical read–only memory disks using metallic island films – preliminary experiments. Appl. Opt. **1993**, *32*(17), 3137–3143.

[241] Ditlbacher, H.; Krenn, J. R.; Lamprecht, B.; Leitner, A.; Aussenegg, F. R. Spectrally coded optical data storage by metal nanoparticles. Opt. Lett. **2000**, *25*(8), 563–565.

[242] Peyser, L. A.; Vinson, A. E.; Bartko, A. P.; Dickson, R. M. Photoactivated fluorescence from individual silver nanoclusters. Science **2001**, *291*(5501), 103–106.

[243] Kawata, Y.; Aoshima, Y.; Egami, C.; Ishikawa, M.; Sugihara, O.; Okamoto, N.; Tsuchimori, M.; Watanabe, O. Light–induced surface modification of urethane–urea copolymer film used as write–once optical memory. Japanese Journal of Applied Physics Part 1 **1999**, *38*(3B), 1829–1831.

[244] Tsujioka, T.; Kume, M.; Irie, M. Superlow–power readout characteristics of photochromic memory. Japanese Journal of Applied Physics Part 1 **1995**, *34*(12A), 6439–6443.

[245] Schellenberg, F. M.; Lenth, W.; Bjorklund, G. C. Technological aspects of frequency–domain data–storage using persistent spectral hole burning. Appl. Opt. **1986**, *25*(18), 3207–3216.

[246] Ortiz, C.; Macfarlane, R. M.; Shelby, R. M.; Lenth, W.; Bjorklund, G. C. Thin–film aggregate color–centers as media for frequency–domain optical storage. Applied Physics **1981**, *25*(2), 87–90.

[247] Macfarlane, R. M.; Shelby, R. M. Photoionization hole burning and nonlinear Zeeman effect in CaF_2–Sm^{2+}. Opt. Lett. **1984**, *9*(12), 533–536.

[248] Macfarlane, R. M.; Meltzer, R. S. Spectral holeburning and the Stark and Zeeman effects in SrF_2–Sm^{2+}. Opt. Commun. **1985**, *52*(5), 320–323.

[249] Yano, R.; Mitsunaga, M.; Uesugi, N. Nonlinear laser spectroscopy of Eu^{3+}:Y_2SiO_5 and its application to time–domain optical memory. J. Opt. Soc. Amer. B **1992**, *9*(6), 992–997.

[250] Zhang, Y.; Shen, X. A.; Kachru, R. Observation of photon echo in Er^{3+}:YAG at 1.527 μm. Opt. Lett. **1997**, *22*(14), 1068–1070.

[251] Breinl, W.; Friedrich, J.; Haarer, D. Logarithmic decay of photochemically induced 2–level systems in an organic glass. Chemical Physics Letters **1984**, *106*(6), 487–490.

[252] Nakatsuka, H.; Sugiyama, H.; Matsumoto, Y. Photon–echoes and persistent hole burning in organic amorphous systems. Journal of Luminescence **1987**, *38*(1-6), 31–33.

[253] Vandenberg, R.; Volker, S. Optical hole–burning in organic glasses. Journal of Luminescence **1987**, *38*(1-6), 25–30.

[254] Drissler, F.; Graf, F.; Haarer, D. Light–induced proton–transfer in dihydroxyanthraquinone as studied by photochemical hole burning. Journal of Chemical Physics **1980**, *72*(9), 4996–5001.

[255] Fujita, K.; Hirao, K.; Tanaka, K.; Soga, N.; Sasaki, H. Persistent spectral hole burning of Eu^{3+} ions in silicate glasses. Japanese Journal of Applied Physics Part 1 **1998**, *37*(4B), 2267–2270.

[256] Moerner, W. E. Molecular electronics for frequency domain optical storage: persistent spectral hole–burning–a review. Journal of Molecular Electronics **1985**, *1*(1), 55–71.

[257] Macfarlane, R. M.; Shelby, R. M. Photo–chemical and population hole burning in the zero–phonon line of a color center – F^{3+} in NaF. Phys. Rev. Lett. **1979**, *42*(12), 788–791.

[258] Macfarlane, R. M. Photon–echo measurements on the trivalent thulium ion. Opt. Lett. **1993**, *18*(22), 1958–1960.

[259] Moerner, W. E., ed. *Persistent Spectral Hole Burning: Science and Applications*. Springer Verlag, New York, **1988**.

[260] Maniloff, E. S.; Johnson, A. E.; Mossberg, T. W. Spectral data storage using rare–earth–doped crystals. MRS Bulletin **1999**, 46–50.

[261] Levenson, M. D.; Macfarlane, R. M.; Shelby, R. M. Polarization–spectroscopy measurement of the homogeneous linewidth of an inhomogeneously broadened color–center band. Phys. Rev. B **1980**, *22*(10), 4915–4920.

[262] Babbitt, W. R.; Lezama, A.; Mossberg, T. W. Optical dephasing, hyperfine–structure, and hyperfine relaxation associated with the 580.8–nm $7f_0$–$5d_0$ transition of europium in Eu^{3+}:Y_2O_3. Phys. Rev. B **1989**, *39*(4), 1987–1992.

[263] Equall, R. W.; Sun, Y.; Cone, R. L.; Macfarlane, R. M. Ultraslow optical dephasing in Eu^{3+}:Y_2SiO_5. Phys. Rev. Lett. **1994**, *72*(14), 2179–2181.

[264] Szabo, A., Frequency selective optical memory. U.S. Patent # 3,896,420, **1975**.

[265] Castro, G.; Haarer, D.; Macfarlane, R. M.; Trommsdorff, H., Frequency selective optical data storage system. U.S. Patent # 4,101,976, **1978**.

[266] Gorokhovskii, A. A.; Kaarli, R. K.; Rebane, L. A. Hole burning in the contour of a pure electronic line in an Shpolskii system. JETP Letters **1974**, *20*, 216–219.

[267] Personov, R. I.; Bykovskaya, L. A. Stable gap in absorption spectra of solid solutions of organic molecules by laser irradiation. Opt. Commun. **1974**, *12*, 191–194.

[268] Mossberg, T. W. Time–domain frequency–selective optical data storage. Opt. Lett. **1982**, *7*(2), 77–79.

[269] Carlson, N. W.; Rothberg, L. J.; Yodh, A. G.; Babbitt, W. R.; Mossberg, T. W. Storage and time reversal of light pulses using photon echoes. Opt. Lett. **1983**, *8*, 483–485.

[270] Mossberg, T. W. Spectral holographic memory promises high areal densities. Data Storage **1996**, 49–52.

[271] Wei, C. J.; Huang, S. H.; Yu, J. Q. 2–photon hole burning and fluorescence–line–narrowing studies on $BaFCl_{0.5}Br_{0.5}$–Sm^{2+} at 77K. Journal of Luminescence **1989**, *43*(3), 161–166.

[272] Reinot, T.; Kim, W. H.; Hayes, J. M.; Small, G. J. New standard for high–temperature persistent–hole–burning molecular materials: Aluminum phthalocyanine tetrasulphonate in buffered hyperquenched glassy films of water. J. Opt. Soc. Amer. B **1997**, *14*(3), 602–608.

[273] Liu, K.; Littman, M. G. Novel geometry for single–mode scanning of tunable lasers. Opt. Lett. **1981**, *6*(3), 117–118.

[274] McNicholl, P.; Metcalf, H. J. Synchronous cavity mode and feedback wavelength scanning in dye–laser oscillators with gratings. Appl. Opt. **1985**, *24*(17), 2757–2761.

[275] Lee, H. W. H.; Huston, A. L.; Gehrtz, M.; Moerner, W. E. Photochemical hole–burning in a protonated phthalocyanine with GaAlAs diode–lasers. Chemical Physics Letters **1985**, *114*(5-6), 491–496.

[276] Wannemacher, R.; Smorenburg, H. E.; Schmidt, T.; Volker, S. Transient hole–burning with a diode–laser – a study of Bacteriochlorophyll–A in a glass on a microsecond time scale. Journal of Luminescence **1992**, *53*(1-6), 266–270.

[277] Harvey, K. C.; Myatt, C. J. External–cavity diode–laser using a grazing–incidence diffraction grating. Opt. Lett. **1991**, *16*(12), 910–912.

[278] Lin, H.; Wang, T.; Mossberg, T. W. Demonstration of 8–Gbit/in^2 areal storage density based on swept–carrier frequency–selective optical memory. Opt. Lett. **1995**, *20*(15), 1658–1660.

[279] Lin, H.; Wang, T.; Wilson, G. A.; Mossberg, T. W. Experimental demonstration of swept–carrier time–domain optical memory. Opt. Lett. **1995**, *20*(1), 91–93.

[280] Rebane, A., Organic frequency–selective materials for ultrafast optical storage and processing. In *Conference on Advanced Optical Memories and Interfaces to Computer Storage*, vol. 3468 of *Proceedings of the SPIE*, **1998** 270–278.

[281] Moerner, W. E.; Chraplyvy, A. R.; Sievers, A. J.; Silsbee, R. H. Persistent nonphotochemical spectral hole dynamics for an infrared vibrational–mode in alkali–halide crystals. Phys. Rev. B **1983**, *28*(12), 7244–7259.

[282] Liu, G. K.; Joubert, M. F.; Cone, R. L.; Jacquier, B. Photon–echo relaxation and hole burning in Tb^{3+}:$LiYF_4$ and $LiTbF_4$. Journal of Luminescence **1987**, *38*(1-6), 34–36.

[283] Huang, J.; Zhang, J. M.; Lezama, A.; Mossberg, T. W. Excess dephasing in photon–echo experiments arising from excitation–induced electronic level shifts. Phys. Rev. Lett. **1989**, *63*(1), 78–81.

[284] Liu, G. K.; Cone, R. L. Laser–induced instantaneous spectral diffusion in Tb^{3+} compounds as observed in photon–echo experiments. Phys. Rev. B **1990**, *41*(10), 6193–6200.

[285] Mitsunaga, M.; Takagahara, T.; Yano, R.; Uesugi, N. Excitation–induced frequency–shift probed by stimulated photon–echoes. Phys. Rev. Lett. **1992**, *68*(21), 3216–3219.

[286] Shen, X. A.; Kachru, R. Optimization of time–domain storage density in the presence of excitation–induced spectral diffusion. Appl. Opt. **1997**, *36*(26), 6692–6695.

[287] Yariv, A. *Quantum Electronics*. 3^{rd} edn., John Wiley & Sons, New York, **1989**.

[288] Devries, H.; Wiersma, D. A. Photophysical and photochemical molecular hole burning theory. Journal of Chemical Physics **1980**, *72*(3), 1851–1863.

[289] Meixner, A. J.; Renn, A.; Wild, U. P. Spectral hole burning and holography. I. Transmission and holographic detection of spectral holes. Journal of Chemical Physics **1989**, *91*, 6728–6736.

[290] Maniloff, E. S.; Altner, S. B.; Bernet, S.; Graf, F. R.; Renn, A. Recording of 6000 holograms by use of spectral hole–burning. Appl. Opt. **1995**, *34*(20), 4140–4148.

[291] Moerner, W. E.; Levenson, M. D. Can single–photon processes provide useful materials for frequency–domain optical storage? J. Opt. Soc. Amer. B **1985**, *2*(6), 915–924.

[292] Kohler, W.; Zollfrank, J.; Friedrich, J. Stability of frequency–domain information bits in amorphous organic materials. J. Appl. Phys. **1989**, *66*(7), 3232–3240.

[293] Wang, G. M.; Equall, R. W.; Cone, R. L.; Leask, M. J. M.; Godfrey, K. W.; Wondre, F. R. Optical dephasing mechanisms in Tm^{3+}:$Y_2Si_2O_7$. Opt. Lett. **1996**, *21*(11), 818–820.

[294] Murase, N.; Horie, K.; Terao, M.; Ojima, M. Theoretical–study of the recording density limit of photochemical hole–burning memory. J. Opt. Soc. Amer. B **1992**, *9*(6), 998–1005.

[295] Babbitt, W. R.; Mossberg, T. W. Quasi–2–dimensional time–domain color memories – process limitations and potentials. Journal of the Optical Society of America B-Optical Physics **1994**, *11*(10), 1948–1953.

[296] Lee, H. W. H.; Gehrtz, M.; Marinero, E. E.; Moerner, W. E. 2–color, photon–gated spectral hole–burning in an organic material. Chemical Physics Letters **1985**, *118*(6), 611–616.

[297] Winnacker, A.; Shelby, R. M.; Macfarlane, R. M. Photon–gated hole burning – a new mechanism using 2–step photoionization. Opt. Lett. **1985**, *10*(7), 350–352.

[298] Macfarlane, R. M. Photon–gated spectral holeburning. Journal of Luminescence **1987**, *38*(1), 20–24.

[299] Lenth, W.; Moerner, W. E. Gated spectral hole–burning for frequency–domain optical–recording. Opt. Commun. **1986**, *58*(4), 249–254.

[300] Moerner, W. E.; Carter, T. P.; Brauchle, C. Fast burning of persistent spectral holes in small laser spots using photongated materials. Appl. Phys. Lett. **1987**, *50*(8), 430–432.

[301] Machida, S.; Horie, K.; Yamashita, T. Photon–gated photochemical hole burning by 2–color sensitization of a photoreactive polymer via triplet–triplet energy–transfer. Appl. Phys. Lett. **1992**, *60*(3), 286–288.

[302] Rebane, A.; Reiss, D.; Renge, I.; Wild, U. P. Non–destructive readout of picosecond time–and–space–domain holograms recorded by photon–gated spectral hole burning. Chemical Physics Letters **1996**, *262*(1-2), 155–160.

[303] Renn, A.; Meixner, A. J.; WIld, U. P.; Burkhalter, F. A. Holographic detection of photochemical holes. Chemical Physics **1985**, *93*, 157–162.

[304] Renn, A.; Wild, U. P. Spectral hole burning and hologram storage. Appl. Opt. **1987**, *26*(19), 4040–4042.

[305] Renn, A.; Meixner, A. J.; Wild, U. P. Spectral hole burning and holography. II. Diffraction properties of two spectrally adjacent holograms. Journal of Chemical Physics **1990**, *92*(5), 2748–2755.

[306] Decaro, C.; Renn, A.; Wild, U. P. Hole burning, Stark–effect, and data–storage. 2. Holographic recording and detection of spectral holes. Appl. Opt. **1991**, *30*(20), 2890–2989.

[307] Rebane, A.; Bernet, S.; Renn, A.; Wild, U. P. Holography in frequency selective media – hologram phase and causality. Opt. Commun. **1991**, *86*(1), 7–13.

[308] Kohler, B.; Bernet, S.; Renn, A.; Wild, U. P. Storage of 2000 holograms in a photochemical hole–burning system. Opt. Lett. **1993**, *18*(24), 2144–2146.

[309] Mitsunaga, M.; Uesugi, N.; Sasaki, H.; Karaki, K. Holographic motion–picture by Eu^{3+}:Y_2SiO_5. Opt. Lett. **1994**, *19*(10), 752–754.

[310] Plagemann, B.; Graf, F. R.; Altner, S. B.; Renn, A.; Wild, U. P. Exploring the limits of optical storage using persistent spectral hole–burning: holographic recording of 12,000 images. Applied Physics B **1998**, *66*(1), 67–74.

[311] Bjorklund, G. C.; Levenson, M. D.; Lenth, W.; Ortiz, C. Frequency–modulation (FM) spectroscopy – theory of lineshapes and signal–to–noise analysis. Applied Physics B **1983**, *32*(3), 145–152.

[312] Huston, A. L.; Moerner, W. E. Detection of persistent spectral holes using ultrasonic modulation. J. Opt. Soc. Amer. B **1984**, *1*(3), 349–353.

[313] Saikan, S.; Kanematsu, Y.; Shiraishi, R.; Nakabayashi, T.; Kushida, T. Hole–burning spectroscopy in dye–doped polymers by spatial modulation technique. Journal of Luminescence **1987**, *38*(1-6), 15–19.

[314] Kroll, S.; Tidlund, P. Recording density limit of photon–echo optical storage with high–speed writing and reading. Appl. Opt. **1993**, *32*(35), 7233–7242.

[315] Ohtsu, M.; Nakagawa, K.; Kourogi, M.; Wang, W. Frequency control of semiconductor–lasers. J. Appl. Phys. **1993**, *73*(12), 1–17.

[316] Drever, R. W. P.; Hall, J. L.; Kowalski, F. V.; Hough, J.; Ford, G. M.; Munley, A. J.; Ward, H. Laser phase and frequency stabilization using an optical–resonator. Applied Physics B **1983**, *31*(2), 97–105.

[317] Seel, S.; Storz, R.; Ruoso, G.; Mlynek, J.; Schiller, S. Cryogenic optical resonators: a new tool for laser frequency stabilization at the 1 Hz level. Phys. Rev. Lett. **1997**, *78*(25), 4741–4744.

[318] Greiner, C.; Boggs, B.; Wang, T.; Mossberg, T. W. Laser frequency stabilization by means of optical self–heterodyne beat–frequency control. Opt. Lett. **1998**, *23*(16), 1280–1282.

[319] Hamilton, M. W. An introduction to stabilized lasers. Contemporary Physics **1989**, *30*(1), 21–33.

[320] Demtroder, W. *Laser Spectroscopy*. 2^{nd} edn., Springer–Verlag, Berlin, **1996**.

[321] Manson, N. B.; Sellars, M. J.; Fisk, P. T. H.; Meltzer, R. S. Hole–burning of rare–earth ions with Khz resolution. Journal of Luminescence **1995**, *64*(1-6), 19–23.

[322] Sellin, P. B.; Strickland, N. M.; Carlsten, J. L.; Cone, R. L. Programmable frequency reference for subkilohertz laser stabilization by use of persistent spectral hole burning. Opt. Lett. **1999**, *24*(15), 1038–1040.

[323] Strickland, N. M.; Sellin, P. B.; Sun, Y.; Carlsten, J. L.; Cone, R. L. Laser frequency stabilization using regenerative spectral hole burning. Phys. Rev. B **2000**, *62*(3), 1473–1476.

[324] Abella, I. D.; Kurnit, N. A.; Hartmann, S. R. Photon echoes. Physical Review **1966**, *141*(1), 391.

[325] Mossberg, T. W. Swept–carrier time–domain optical memory. Opt. Lett. **1992**, *17*(7), 535–537.

[326] Shen, X. A.; Nguyen, A. D.; Perry, J. W.; Huestis, D. L.; Kachru, R. Time–domain holographic digital memory. Science **1997**, *278*(5335), 96–100.

[327] Jefferson, C. M.; Meixner, A. J. Frequency–domain measurements of spectral hole patterns burned with phase–coherent pulses. Chemical Physics Letters **1992**, *189*(1), 60–66.

[328] Merkel, K. D.; Babbitt, W. R. Optical coherent–transient true–time–delay regenerator. Opt. Lett. **1996**, *21*(15), 1102–1104.

[329] Mitsunaga, M.; Yano, R.; Uesugi, N. Spectrally programmed stimulated photon–echo. Opt. Lett. **1991**, *16*(4), 264–266.

[330] Schwoerer, H.; Erni, D.; Rebane, A. Holography in frequency–selective media. III. spectral synthesis of arbitrary time–domain pulse shapes. J. Opt. Soc. Amer. B **1995**, *12*(6), 1083–1093.

[331] Rebane, A. K.; Kaarli, R. K.; Saari, P. M. Dynamic picosecond holography produced by means of photochemical hole burning. Jetp Letters **1983**, *38*(7), 383–386.

[332] Kim, M. K.; Kachru, R. Long–term image storage and phase conjugation by a backward–stimulated echo in Pr^{3+}–LaF_3. J. Opt. Soc. Amer. B **1987**, *4*(3), 305–308.

[333] Kim, M. K.; Kachru, R. Storage and phase conjugation of multiple images using backward–stimulated echoes in Pr^{3+}–LaF_3. Opt. Lett. **1987**, *12*(8), 593–595.

[334] Hesselink, W. H.; Wiersma, D. A. Picosecond photon–echoes stimulated from an accumulated grating. Phys. Rev. Lett. **1979**, *43*(27), 1991–1994.

[335] Asaka, S.; Nakatsuka, H.; Fujiwara, M.; Matsuoka, M. Accumulated photon–echoes with incoherent–light in Nd^{3+}–doped silicate glass. Phys. Rev. A **1984**, *29*(4), 2286–2289.

[336] Saikan, S.; Kishida, T.; Imaoka, A.; Uchikawa, K.; Furusawa, A.; Oosawa, H. Optical memory based on heterodyne–detected accumulated photon–echoes. Opt. Lett. **1989**, *14*(16), 841–843.

[337] Mitsunaga, M.; Uesugi, N. 248–bit optical–data storage in Eu^{3+}–$YAlO_3$ by accumlated photon–echoes. Opt. Lett. **1990**, *15*(3), 195–197.

[338] Babbitt, W. R.; Bell, J. A. Coherent transient continuous optical processor. Appl. Opt. **1994**, *33*(8), 1538–1548.

[339] Zhu, M.; Babbitt, W. R.; Jefferson, C. M. Continuous coherent transient optical processing in a solid. Opt. Lett. **1995**, *20*(24), 2514–2516.

[340] Merkel, K. D.; Babbitt, W. R. Chirped–pulse programming of optical coherent transient true–time delays. Opt. Lett. **1998**, *23*(7), 528–530.

[341] Merkel, K. D.; Babbitt, W. R.; Anderson, K. E.; Wagner, K. H. Variable–time–delay optical coherent transient signal processing. Opt. Lett. **1999**, *24*(20), 1386–1388.

[342] Shen, X. A.; Kachru, R. Optical header recognition by spectroholographic filtering. Opt. Lett. **1995**, *20*(24), 2508–2510.

[343] Wang, T.; Lin, H.; Mossberg, T. W. Experimental demonstration of temporal–waveform–controlled spatial routing of optical beams by spatial–spectral filtering. Opt. Lett. **1995**, *20*(24), 2541–2543.

[344] Merkel, K. D.; Babbitt, W. R. Optical coherent transient header/data isolation technique. Opt. Lett. **1996**, *21*(1), 71–73.

[345] Harris, T. L.; Sun, Y.; Cone, R. L.; Macfarlane, R. M.; Equall, R. W. Demonstration of real–time address header decoding for optical data routing at 1536 nm. Opt. Lett. **1998**, *23*(8), 636–638.

[346] Bai, Y. S.; Babbitt, W. R.; Carlson, N. W.; Mossberg, T. W. Real–time optical waveform convolver cross correlator. Appl. Phys. Lett. **1984**, *45*(7), 714–716.

[347] Shen, X. A.; Bai, Y. S.; Kachru, R. Reprogrammable optical matched–filter for biphase–coded pulse–compression. Opt. Lett. **1992**, *17*(15), 1079–1081.

[348] Ollikainen, O. Optical implementation of quadratic associative memory by use of persistent spectral hole–burning media. Appl. Opt. **1993**, *32*(11), 1943–1947.

[349] Babbitt, W. R.; Mossberg, T. W. Spatial routing of optical beams through time–domain spatial–spectral filtering. Opt. Lett. **1995**, *20*(8), 910–912.

[350] Merkel, K. D.; Babbitt, W. R. Optical coherent transient continuously programmed continuous processor. Opt. Lett. **1999**, *24*(3), 172–174.

[351] Rebane, A.; Drobizhev, M.; Sigel, C.; Ross, W.; Gallus, J. Ultrafast optical processing with photon echoes. Journal of Luminescence **1999**, *83-84*, 325–333.

[352] Kroll, S.; Elman, U. Photon–echo–based logical processing. Opt. Lett. **1993**, *18*(21), 1834–1836.

[353] Ross, W.; Drobizhev, M.; Sigel, C.; Rebane, A. Demonstration of an ultrafast logic gate by interference of coherent transients. Laser Physics **1999**, *9*(5), 1102–1107.

[354] Macfarlane, R. M.; Harris, T. L.; Sun, Y.; Cone, R. L.; Equall, R. W. Measurement of photon echoes in Er:Y_2SiO_5 at 1.5 μm with a diode laser and an amplifier. Opt. Lett. **1997**, *22*(12), 871–873.

[355] Bai, Y. S.; Babbitt, W. R.; Mossberg, T. W. Coherent transient optical pulse–shape storage recall using frequency–swept excitation pulses. Opt. Lett. **1986**, *11*(11), 724–726.

[356] Lin, H.; Wang, T.; Wilson, G. A.; Mossberg, T. W. Heterodyne–detection of swept–carrier frequency–selective optical memory signals. Opt. Lett. **1995**, *20*(8), 928–930.

[357] Johnson, A. E.; Maniloff, E. S.; Mossberg, T. W. Spatially distributed spectral storage. Opt. Lett. **1999**, *24*(21), 1526–1528.

[358] Bai, Y. S.; Kachru, R. Coherent time–domain data–storage with a spread–spectrum generated by random biphase shifting. Opt. Lett. **1993**, *18*(14), 1189–1191.

[359] Shen, X. A.; Kachru, R. Coherent saturation removal in time–domain optical memory by storage of frequency–chirped data pulses. Opt. Lett. **1993**, *18*(22), 1967–1969.

[360] Shen, X. A.; Kachru, R. Use of biphase–coded pulses for wide–band data–storage in time–domain optical memories. Appl. Opt. **1993**, *32*(17), 3149–3151.

[361] Shen, X. A.; Kachru, R. Experimental demonstration of impulse–equivalent time–domain optical memory. Opt. Lett. **1996**, *21*(24), 2020–2022.

[362] Shen, X. A.; Hartman, R.; Kachru, R. Impulse–equivalent time–domain optical memory. Opt. Lett. **1996**, *21*(11), 833–835.

[363] Burckhardt, C. B. Use of a random phase mask for the recording of Fourier transform holograms of data masks. Appl. Opt. **1970**, *9*(3), 695–700.

[364] Iwamoto, A. Artificial diffuser for Fourier transform hologram recording. Appl. Opt. **1980**, *19*(2), 215–221.

[365] Brauer, R.; Wojak, U.; Wyrowski, F.; Bryngdahl, O. Digital diffusers for optical holography. Opt. Lett. **1991**, *16*(18), 1427–1429.

[366] Azadeh, M.; Cornish, C. S.; Babbitt, W. R.; Tsang, L. Efficient photon echoes in optically thick media. Phys. Rev. A **1998**, *57*(6), 4662–4668.

[367] Wang, T.; Greiner, C.; Mossberg, T. W. Photon echo signals: beyond unit efficiency. Opt. Commun. **1998**, *153*(4-6), 309–313.

[368] Cornish, C. S.; Babbitt, W. R.; Tsang, L. Demonstration of highly efficient photon echoes. Opt. Lett. **2000**, *25*(17), 1276–1278.

[369] Mohan, R. K.; Elman, U.; Tian, M. Z.; Kroll, S. Regeneration of photon echoes with amplified photon echoes. Opt. Lett. **1999**, *24*(1), 37–39.

[370] Mitsunaga, M.; Kim, M. K.; Kachru, R. Degenerate photon–echoes – simultaneous storage of multiple optical–data. Opt. Lett. **1988**, *13*(6), 536–538.

[371] Kachru, R.; Bai, Y. S.; Shen, X. A. Time–frequency domain optical storage in rare–earth–doped materials. Advanced Materials **1994**, *6*(10), 791–793.

[372] Shen, X. A.; Kachru, R. High–speed holographic recording of 500 images in a rare earth doped solid. Journal of Alloys and Compounds **1997**, *250*(1-2), 435–438.

[373] Rebane, A.; Drobizhev, M.; Sigel, C. Single femtosecond exposure recording of an image hologram by spectral hole burning in an unstable tautomer of a phthalocyanine derivative. Opt. Lett. **2000**, *25*(22), 1633–1635.

[374] Weiner, A. M.; Heritage, J. P.; Kirschner, E. M. High–resolution femtosecond pulse shaping. J. Opt. Soc. Amer. B **1988**, *5*(8), 1563–1572.

[375] Weiner, A. M.; Leaird, D. E.; Reitze, D. H.; Paek, E. G. Spectral holography of shaped femtosecond pulses. Opt. Lett. **1992**, *17*(3), 224–226.

[376] Weiner, A. M.; Leaird, D. E.; Reitze, D. H.; Paek, E. G. Femtosecond spectral holography. IEEE J. Quantum Electron. **1992**, *28*(10), 2251–2261.

[377] Sun, P. C.; Oba, K.; Mazurenko, Y. T.; Fainman, S. Y. Space–time processing with photorefractive volume holography. Proc. IEEE **1999**, *87*(12), 2086–2097.

[378] Marom, D.; Panasenko, D.; Sun, P. C.; Fainman, Y. Femtosecond–rate space–to–time conversion. J. Opt. Soc. Amer. B **2000**, *17*(10), 1759–1773.

[379] Weiner, A. M. Femtosecond pulse processing. Optical and Quantum Electronics **2000**, *32*(4-5), 473–487.

[380] Marom, D. M.; Panasenko, D.; Sun, P. C.; Fainman, Y. Spatial–temporal wave mixing for space–time conversion. Opt. Lett. **1999**, *24*(8), 563–565.

[381] Konishi, T.; Ichioka, Y. Ultrafast image transmission by optical time–to–two–dimensional–space–to–time–to–two–dimensional–space conversion. J. Opt. Soc. Amer. A **1999**, *16*(5), 1076–1088.

[382] Marom, D. M.; Panasenko, D.; Sun, P. C.; Fainman, Y. Linear and nonlinear operation of a time–to–space processor. J. Opt. Soc. Amer. A **2001**, *18*(2), 448–458.